ADVANCED MATERIALS

Energy Level Alignment and Interfacial Electronic Structures at Organic/Metal and Organic/Organic Interfaces**

By Hisao Ishii, Kiyoshi Sugiyama, Eisuke Ito, and Kazuhiko Seki*

1. Introduction

Recently there has been much interest in electronically functional organic materials with respect to various applications. In many cases, the function originates at interfaces. Some examples are shown in Figure 1 with schematic energy diagrams: 1 a) shows an organic electroluminescent (EL) device in which electrons (e^-) and holes (h^+) are injected from the electrodes into the electron transport layer (ETL) and hole transport layer (HTL), respectively. These carriers recombine to emit light, possibly in another emission layer.[1,2] 1 b) depicts spectral sensitization in silver halide photography. In this process, an electron is photoexcited in an organic dye molecule adsorbed on an Ag halide (AgX) surface, and is injected into the conduction band of Ag halide, leading to sensitization.[3] 1 c) shows an organic solar cell: Photoformed electron–hole pairs in the organic layer are separated in the bent band region accompanied by the Schottky barrier.[4]

Thus the elucidation of the interfacial electronic structure forms the basis for understanding and improving the performance of these devices. In particular, the organic/metal and organic/organic interfaces have attracted much interest in relation to the rapid development of the organic EL devices. In addition, metal/organic interfaces will be important in the wiring of future molecular devices.

The subject of interfacial electronic structure can be roughly divided into two aspects: 1, the energy level alignment at the interface; and 2, the band bending in a thicker region,[5] as shown in Figure 1c. The former is important in carrier injection (e.g., in EL devices or spectral sensitization), while the latter is essential for carrier separation (e.g., in a solar cell).

In this article, we will review recent progress in the understanding of the interfacial electronic structures, focusing on the results of ourselves and other workers in energy level alignment at the interface. Band bending will also be briefly discussed. In particular, we point out the invalidity of the traditional assumption of a common vacuum level (VL), which has been widely used in the field of organic devices for estimating the interfacial electronic structure.[6–9] This situation probably arises from conceptual confusion caused by the lack of communication within the field of surface science.

In order to improve this situation, we reexamine the basic concepts and summarize the present status of understanding about electronic structures of interfaces (including organic materials) in the interdisciplinary forum of *Advanced Materials*. The emphasis is more on molecular materials than polymers, since the former are easier to characterize and are more suitable for examining the fundamental aspects of interfacial electronic structure, as discussed in Section 2.4.

Such conceptual aspects are addressed in Section 2. In Section 3, recent results about energy level alignment at organic/metal and organic/organic interfaces are reviewed, including discussion about band bending. Future prospects are presented in Section 4. Those well-grounded in conceptual aspects can pass over the next section and go directly to Section 3.

The references are not intended to be comprehensive, but rather to highlight the important aspects. Therefore the authors apologize in advance to the authors of papers not

[*] Prof. K. Seki
Research Center for Materials Science and Department of Chemistry
Graduate School of Science, Nagoya University
Furocho, Chikusa-ku, Nagoya 464-8602 (Japan)
Dr. H. Ishii, Dr. K. Sugiyama[+]
Department of Chemistry, Graduate School of Science
Nagoya University
Furocho, Chikusa-ku, Nagoya 464-8602 (Japan)
Dr. E. Ito
Venture Business Laboratory, Nagoya University
Furocho, Chikusa-ku, Nagoya 464-8602 (Japan)
[+] Present address: Tsukuba Research Center, Mitsubishi Chemical Corporation, Ami, Inashiki, Ibaraki 300-0332 (Japan)

[**] The authors thank Drs. S. Narioka, T. Miyazaki, S. Hasegawa, S. Egusa, and T. Sasaki, Messrs. D. Yoshimura, H. Oji, N. Hayashi, and T. Yokoyama, and Profs. Y. Ouchi, N. Ueno, Y. Harima, and K. Yamashita for the collaboration in our work described here. They also acknowledge helpful discussions with Profs. A. Kahn, Y. Gao, M. Pope, W. R. Salaneck, M. Tsukada, N. Karl, and E. Umbach, Drs. W. Riess, C. W. Tang, W. Widdra, and S. Alvarado, and thank Profs. Y. Gao, and A. Kahn, Drs. V. E. Choong, R. Schlaf and S. Alvarado, and Mr. M. Koch for the communication of their results prior to publication. Our work was supported in part by the Grant-in-Aid for Scientific Research from the Ministry of Education, Science, Sports, and Culture of Japan (Nos. CE072004, 10146102, and 10440205), Venture Business Laboratory Program Advanced Nanotechnology and Joint Studies Program of Center for Integrated Research in Science and Engineering of Nagoya University, and Joint Studies Program of UVSOR facility of Institute for Molecular Science.

  0935-9648/99/0806-0605 $ 17.50+.50/0

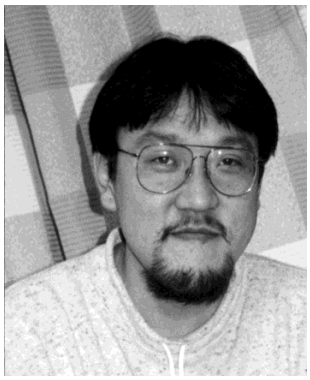

Hisao Ishii was born in Hyogo, Japan, in 1962. He received his M.S. and Ph.D. degrees in chemistry from the University of Tokyo, in 1988 and 1991, respectively. His thesis research focused on the metastable atom electron spectroscopy of clean and adsorbate-covered silicon surfaces. In 1991, he joined the Solid State Chemistry Laboratory, Nagoya University, Nagoya, Japan, where he is currently working as a research associate. His current research interests include electron spectroscopy of functional organic materials, electronic structure of organic/inorganic interfaces, and molecular orientation of thin organic films. From 1995 to 1997, he was on leave at the Institute for Molecular Science, Okazaki, Japan, to investigate the electronic structure of organic/metal interfaces with synchrotron radiation.

Kiyoshi Sugiyama was born in 1970 in Chiba, Japan. He studied at the Tokyo Institute of Technology with Prof. Takakazu Yamamoto (1993–1994) and at Nagoya University with Prof. Kazuhiko Seki (1992, 1995–1997), where he wrote his Ph.D. thesis entitled The UV Photoemission Study of the Electronic Structures of Organic Electroluminescent Devices*. In 1998, he joined Tsukuba Research Center, Mitsubishi Chemical Corporation, and is involved in research on interfacial electronic structures of opto-electronic devices.*

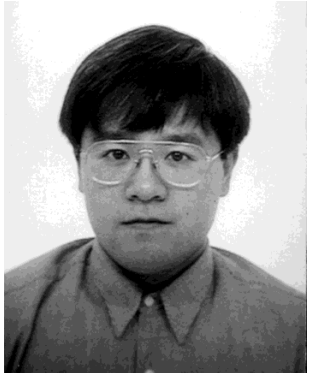

Eisuke Ito was born in Toyohashi, Japan, on May 17, 1969. He receieved his Ph.D. degree from Nagoya University in 1997, since when he has been a Post-Doctoral Research Associate at the Venture Business Laboratory, Nagoya University, Japan. His current interests are focused on the interfacial electronic structures of organic/metal interfaces and molecular orientaion of organic thin films on clean metals.

Kazuhiko Seki was born in 1947 in Ashiya, Japan. He graduated from the Department of Chemistry, University of Tokyo (1970) and obtained his Ph.D. degree at the Institute for Solid State Physics (ISSP), University of Tokyo (1975), under the guidance of Profs. H. Akamatu and H. Inokuchi, who were pioneers in the field of organic semiconductors in Japan. Here he began his study of organic materials by UPS. He then moved to Okazaki (Institute for Molecular Science IMS, 1978) and to Hiroshima (Department of Materials Science, Hiroshima University, 1986), where he learned the technique of NEXAFS from Prof. T. Ohta for studying molecular orientation. In 1983 he visited the HASYLAB (Hamburg) with the late Prof. E.-E. Koch to perform UPS studies of organic materials using synchrotron radiation, and later constructed a UPS beamline at the synchrotron radiation facility UVSOR at IMS, which is dedicated to the study of organic materials. In 1991 he moved to Nagoya (Department of Chemistry, Nagoya University, 1991) as a full professor to open the Solid State Chemistry Laboratory. In April 1998, he joined the newly established Research Center for Materials Science (RCMS) of Nagoya University. His current research interest is in functional organic materials such as organic semiconductors, liquid crystals, functional and fundamental polymers, dyes, and fullerenes. In particular, he carries out characterization of ultrathin films, surfaces, and interfaces of these materials in relation to their function.

  0935-9648/99/0806-0606 $ 17.50+.50/0

ADVANCED MATERIALS

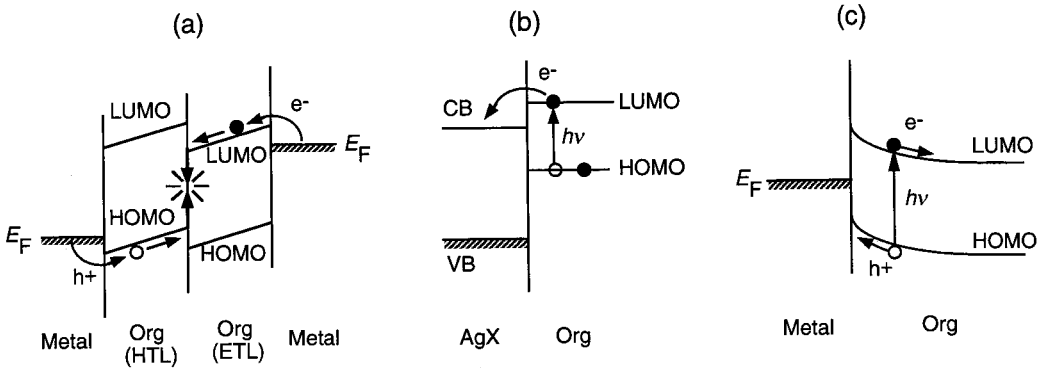

Fig. 1. Energy diagrams of organic electronic devices with functions originating at interfaces. a) EL device. b) Spectral sensitization in silver halide photography. c) Organic solar cell using metal/organic Schottky barrier.

cited here. Also it is evident that much more work is needed to obtain full understanding of the interfacial electronic structure. In this respect, the following can be viewed as a report of the present status in this rapidly developing young field.

2. Conceptual Aspects: Factors Determining Interfacial Electronic Structures

2.1. The Electronic Structure of an Organic Solid

We start the examination of the basic concepts with the electronic structure of a hydrogen atom (Fig. 2a). The ordinate is the electron energy. The potential well is the Coulombic potential by the atomic nucleus. Various atomic orbitals (AOs) are formed in this well, and an electron occupies the lowest 1s orbital. The horizontal part of the potential well is the vacuum level (VL), above which the electron can escape from the atom.

Figure 2b shows the electronic structure of a polyatomic molecule or a single polymer chain. The effective potential well of an electron is formed by the atomic nuclei and other electrons. The wells of the nuclei are merged in the upper part to form a broad well. Deep AOs are still localized in the atomic potential well (core levels), but the upper AOs interact to form delocalized molecular orbitals (MOs). The outermost horizontal part of the potential well is again the VL. The energy separations from the highest occupied MO (HOMO) or lowest unoccupied MO (LUMO) to the VL are the gas phase ionization energy (I_g) or the electron affinity (A_g) of the molecule, respectively.

When molecules or polymer chains come together to form an organic solid, the electronic structure becomes like Figure 2c. Since the molecules interact only by the weak van der Waals interaction, the top part of the occupied valence states (or valence band) and the lower unoccupied states (conduction band) are usually localized in each molecule, with narrow intermolecular band widths of < 0.1 eV.[10,11] Thus the electronic structure of an organic solid largely preserves that of a molecule or a single chain, and the validity of usual band theory (which assumes itinerant electrons) is often limited.[12] The top of the occupied state and the bottom of the unoccupied state are often noted as HOMO and LUMO, reflecting the correspondence with the molecular state.

The situation in Figure 2c is often simplified to those in Figure 2d and Figure 2e. Although the VL in Figure 2e is

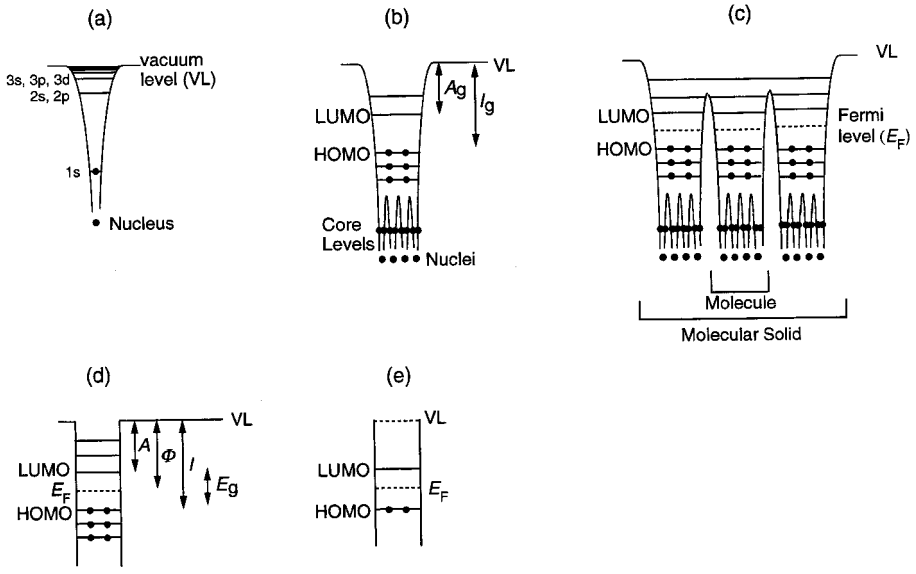

Fig. 2. Electronic structure represented with potential wells. a) Hydrogen atom. b) Polyatomic molecule. c) Organic solid. d) and e) Simplification of (c). I_g: gas phase ionization energy, A_g: gas phase electron affinity, I: solid state ionization energy, A: solid state electron affinity, Φ: work function, and E_g: HOMO–LUMO bandgap.

  0935-9648/99/0806-0607 $ 17.50+.50/0

shown as if it is inside the solid, it is actually on the outside. In Figures 2c–e, the Fermi level is also indicated (E_F). Since the electrons fill the energy levels following the Fermi statistics, the concept of Fermi level is always valid.

The ionization energy (I) and electron affinity (A) of the solid are defined as the energy separation of the HOMO and the LUMO from the VL, as in the case of a molecule (see Fig. 2d). The values of I and A are different from those of an isolated molecule due to a multielectronic effect. In the condensed state, the electronic polarization in the molecules surrounding the ionized molecule stabilizes the ion (polarization energies P_+ and P_- for the hole and the electron, respectively), leading to a lowering of the ionization energy and an increase in electron affinity from those in the gas phase.[11,13–15] The work function Φ of the solid is defined as the energy separation between the Fermi level and the VL.

The value of I can be determined by techniques such as UV photoemission spectroscopy (UPS) and photoemission yield spectroscopy (PEYS), which are described in Section 3.[11,15,16] The recent development of a commercial PEYS instrument offered a conventional method of measuring I of compounds insensitive to air under atmospheric conditions.[17] The entire valence electronic structures can also be studied by UPS and X-ray photoelectron spectroscopy (XPS).[9,16] The value of A can in principle be determined by inverse photoemission spectroscopy (IPES),[18–21] but it is often hindered by the radiation damage of the sample. Thus the value of A is usually estimated from the values of I, and the HOMO–LUMO gap deduced from optical measurements (optical bandgap E_g^{opt}). More precisely, E_g^{opt} is, in general, different from the true bandgap (the energy required for forming a free electron–hole pair) due to the Coulombic stabilization energy, C, between the electron–hole pair (excitonic effect) and the polarization energies of the electron and the hole.[22] Only when C is incidentally equal to $P_+ + P_-$, does E_g^{opt} become equal to the true bandgap. Information about the work function, Φ, can be obtained by the UPS[23] and Kelvin probe methods,[24] although the physical interpretation of the observed value needs some care, as descried in Section 3. We also note that critical selection of various energy parameters is available for representative organic semiconductors.[25]

2.2. Definition of the Vacuum Level

When an isolated electron is at rest in a vacuum, it is said to be at the VL. The VL for an electron at rest at infinite distance from the system is often taken as an invariant energy reference. We will call this vacuum level at infinite distance, and denote it as VL(∞). On the other hand, the VL of a solid involved in the measurements of I, A, and Φ corresponds to the energy of an electron at rest just outside the solid, and it is still affected by the potential of the solid.[24, 26] We refer to this as vacuum level at surface, and denote it as VL(s). Thus the experimentally determined VL is not that for an electron at infinite distance, and it cannot be used as an invariant reference level. There has often been misunderstanding about this point, with confusion between VL(s) and VL(∞).

The effect of the solid on VL(s) is most convincingly demonstrated by the well-known dependence of the work function on the surface of a single crystal. For example, the work function of a tungsten single crystal is 4.63, 5.25, and 4.47 eV for the (100), (110), and the (111) surfaces, respectively, as shown in Figure 3.[27] Since the Fermi level is a common level inside the solid, this dependence is due to the energy difference of an electron just outside of the solid, or VL(s), as shown in Figure 4a.

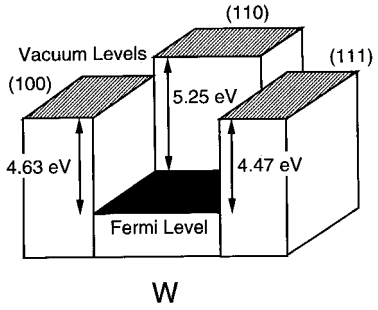

Fig. 3. Dependence of the work function of a tungsten single crystal on the crystalline surface. The energy of the vacuum level at the surface VL(s) is different for the (100), (110), and (111) surfaces. The values of work functions are taken from the paper by Strayer et al. [27].

For a metal, the difference between the energies of VL(∞) and VL(s) is mostly due to the surface dipole layer formed by the tailing of the electron cloud at the surface, as shown by the electron density distribution in Figure 4b.[28,29] The tailing of the negatively charged electron cloud into vacuum makes the vacuum side negative, while the lack of electrons inside the surface makes the bulk side positive.

For an electron at a distance x from a dipole layer of finite extension, with a representative length L (Fig. 4d), the potential energy $V(x)$ by the dipole layer becomes as shown in Figure 4c. For a very small distance $x \ll L$, the dipole layer can be regarded to be infinitely extended. In such a case, the potential energy forms a step function across the dipole layer, and $V(x)$ at each side is independent of x.[30] When the electron is separated from the dipole layer to make $x \gg L$, the dipole layer can be regarded as a point dipole, and the potential decreases as x^{-2}.[30]

Such contribution from the surface dipole layer makes the potential energy for an electron in and out of a metal as shown in Figure 4a. The flat portion of the potential just outside the surface in Figure 4a is the region of $x \ll L$. As the distance from the surface becomes larger than the extension of the sample surface ($x \gg L$), the effect of the surface dipole layer diminishes, and the energy of free electron gradually converges to a common value, which corresponds to VL(∞). The dependence of the work function on the surface can be ascribed to the difference in the tailing of the electron cloud at different surfaces.

For organic solids, the existence of a surface dipole layer comparable to that of a metal surface has not yet been

  0935-9648/99/0806-0608 $ 17.50+.50/0

ADVANCED MATERIALS

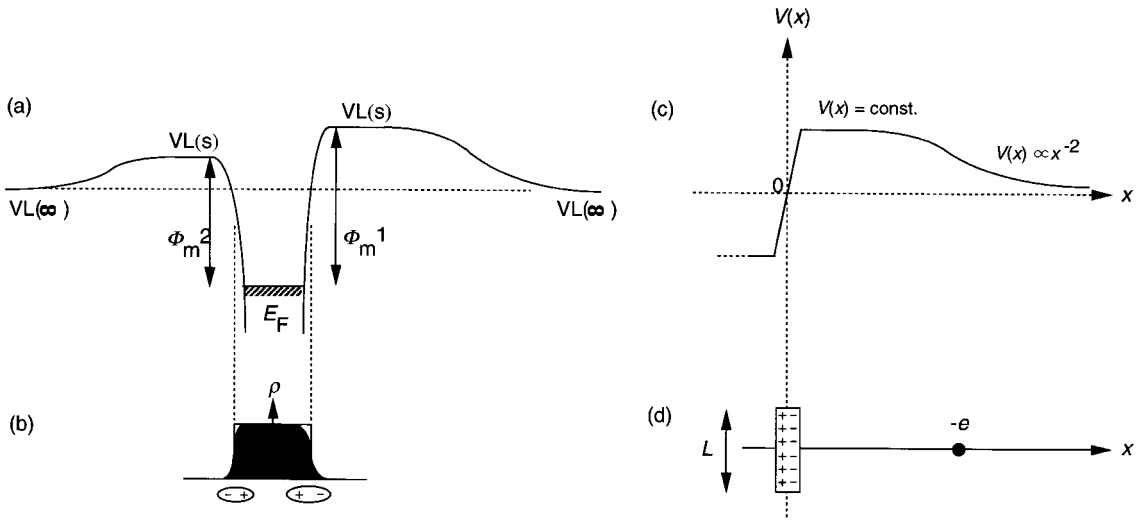

Fig. 4. a) Potential surface for an electron in and out of a metal crystal. E_F: Fermi level, VL(s): vacuum level at the surface, VL(∞): vacuum level at infinite distance, Φ_m^1 and Φ_m^2: work functions of different crystal surfaces. b) Electron density in the metal, with tailing at the surface to form a surface dipole layer. Note that the degree of tailing depends on the surface. c) Electron and dipole layer with a representative extension L with the distance x between them. d) The potential energy of the electron by the dipole layer in (c).

seriously examined by experiments. At least for solids formed by nonpolar molecules, we can speculate that it will be not so large for a free surface.

2.3. Interfacial Electronic Structure

An interface between the solids of two materials can be formed either by: a) the contact of two solids, or b) the deposition of one material on the solid surface of the other.

The studies of interfaces in these views have been developed rather separately in the fields of electronic devices and surface science, at least for organic molecules. In the following, we attempt to combine the knowledge from these studies. Although we will primarily examine a metal/organic interface, the results can be easily extended to other types (organic/organic, organic/semiconductor etc.) of interfaces, with appropriate cautions.

2.3.1. Energy Level Alignment at the Interface

Figures 5a and b illustrate the change in the potential well and the electronic states at the interface formation between a metal and an organic solid respectively. When a metal and an organic solid are far away, their energy levels are aligned sharing VL(∞), as shown in Figure 5a. When the solids come into contact without rearrangement of the electric charge, the organic layer is now in the potential of the surface dipole of the metal, and its energy levels are raised to have a common VL(s) in an extremely narrow interfacial gap, as shown in Figure 5b. In the actual contact, the two potential wells may be merged as indicated by the broken line, but it is often represented as shown by the solid line. In this sense, the vacuum level at the interface is a hypothetical concept to make the discussion easy. The situation in Figure 5b is often represented as Figure 5c. Here we omit the lines of VL(∞), since the confusion between VL(s) and VL(∞) has been removed.

In the actual systems, a dipole layer may be formed right at the interface, due to various origins such as charge transfer across the interface, redistribution of electron cloud, interfacial chemical reaction, and other types of rearrangement of electronic charge.[24,31] We should recognize that this is an additional dipole layer, when there is already a dipole layer at the free surface as in the case of metal surfaces depicted in Figure 4b.

With such interfacial dipole formation, there will be an abrupt shift of the of the potential across the dipole layer as shown in Figure 4d,[30] leading to a shift of virtual VL Δ at the interface, as shown in Figure 5d. The value of Δ is determined by the magnitude of the dipole. This leads to the shift in VL in the organic layer at the right-hand side in Figure 5d from that of the metal at the left-hand side. Nielsen pointed out the importance of such interfacial dipole layer in 1974,[32] but not much experimental work has been carried out. Consequently, this factor has often been neglected in the field of organic devices, possibly again because of the naive confusion between VL(s) and VL(∞).

On the other hand, this possible shift of the VLs is well-known in the field of surface science at the adsorption and deposition of molecules on metal surfaces.[24,31] It is usually called the change in the work function (or surface potential) of the metal, and extensive studies have been carried out for small molecules.[31] Following the custom in this field, we will take Δ to be positive when the VL is raised by deposition.

In principle, controlled deposition in ultrahigh vacuum (UHV) is a convenient way to examine the interfacial electronic structure.[33] Unfortunately, most of such studies for organic compounds have been limited in the thickness region of submonolayer to several layers, and not much work

  0935-9648/99/0806-0609 $ 17.50+.50/0

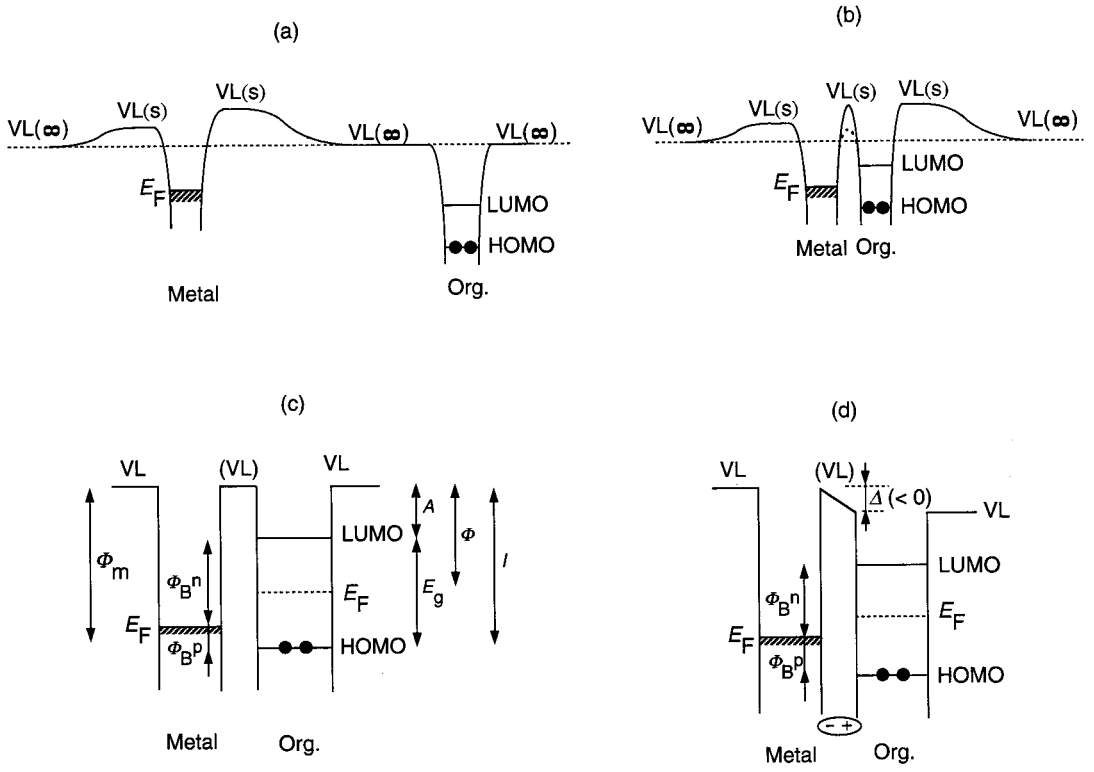

Fig. 5. a) Electronic structure of a metal and an organic solid at infinite distance. b) Contact of a metal and a thin organic solid layer. The organic layer is within the electric field of the surface dipole layer of the metal, and the interfacial VL is common. When the two solids come into real contact, the actual potential well may become as shown by the broken line. c) Schematic representation of (a) assuming common (virtual) VLs at the interface. Φ_B^n and Φ_B^p denote the injection barriers for electron and hole. Other symbols are the same as in Figure 2. d) Interfacial energy diagram with a shift of VL Δ at the interface due to dipole layer formation. In this figure, the organic side is charged positive, making this side more comfortable (low energy) for an electron, and making the sign of Δ negative.

has been carried out in interfaces with thicker organic layers, which can be regarded as solids. Also, most studies of the work function change were carried out for small molecules, and electronically functional large molecules have not been greatly examined, although there were some exceptions.[34–36]

2.3.2. Band Bending in the Organic Layer

For an interface with a thick organic layer, band bending should also be considered. In general, work functions for the metal and the organic layer are different, and the interfaces in Figure 5c and Figure 5d are not in electrical equilibrium, where the Fermi levels would be at the same energy. If the total number of the available mobile carriers in the organic layer is sufficiently large, there will be a charge redistribution around the interface within a reasonably short time of an experiment. In the case of Figure 5c, for example, the work function of the metal is larger than that of the organic layer, and the metal is more comfortable for an electron. As a result, some electrons may move from the organic layer to the metal, leading to the negative and positive charging of the metal and the organic layer, respectively. This charging makes the metal less comfortable for the negatively charged electron. Also, there may be a redistribution of mobile charge carriers in the organic layer. This flow and distribution of charge continues until the Fermi levels are aligned between the metal and the bulk of the organic layer.

In such a redistribution of the charges, the potential distribution at the interfacial region is governed by the Poisson equation, which expresses the relation between the charge and potential distributions. As a result, a diffusion layer with band bending forms to align the Fermi energies of the two solids, with a built in potential V_{bi} in the organic layer.[5,10,37] This corresponds to the work function and is shown in Figures 6a and b, for the cases with and without the interfacial dipole layer, respectively. The thickness of the diffusion layer W depends on factors such as V_{bi}, the dielectric constant of the organic layer ε, and the spatial distribution of the available donor or acceptor levels.[5] For example, W is of the order of 10 μm in the case of Si with a dopant concentration of 10^{16} cm^{-3}, $\varepsilon = 12$, and $V_{bi} = 0.5$ eV.[5]

Here we note that such alignment of the Fermi level by band bending in Figures 6a and b is possible only when sufficient number of mobile charge carriers are available, either in a rather thick organic layer or organic layer with good semiconducting character. Such carriers may be available by extrinsic origin in polymers or materials under air, but are not expected in a thoroughly purified molecular layer prepared

  0935-9648/99/0806-0610 $ 17.50+.50/0

ADVANCED MATERIALS

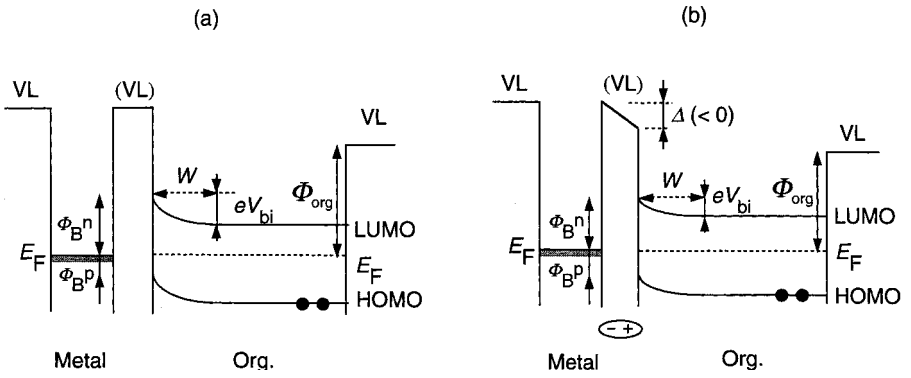

Fig. 6. Interfacial energy diagram with band bending [5]. The energy levels are bent by the charge redistribution in the organic layer to achieve the electrical equilibrium with the alignment of the Fermi levels of the two sides. This leads to the buildup of built-in potential V_{bi} within a diffusion layer of thickness W. a) and b) correspond to the cases without and with VL shift in Figures 5c and d, respectively.

under UHV, since the HOMO–LUMO separation is usually much larger than the thermal energy. Thus for a very thin layer of molecular material in UHV, nearly-flat-band situations in the interfacial region are expected, as shown in Figures 5c and d,[9,38,39] and the alignment of the Fermi level is not easily established (although there is a report that Fermi level alignment is achieved within 10 nm even for a molecular solid layer in UHV[40]) in the short time accessible in an experiment. Thus we can study the energy level alignment right at the interface by using a thin deposited layer up to, say, a few nanometers thick, assuming almost-flat-band as a first-order approximation.

2.3.3. Carrier Injection Barriers

In the cases of Figure 5c and Figure 6a without interfacial dipole layer formation, the (virtual) VL at the interface is common, and the barrier heights of carrier injection at the interface for hole (Φ_B^p) and electron (Φ_B^n) are given in Equations 1 and 2, respectively, where Φ_m is the work function of the metal and E_g is the bandgap of the organic layer. Equations 1 and 2 comprise the Schottky–Mott rule,[41] and correspond to the case of simple contact. When this rule applies, we can deduce the barrier height from the values of Φ_m and I determined by techniques like UPS and PEYS.

$$\Phi_B^p = I - \Phi_m, \tag{1}$$

$$\Phi_B^n = \Phi_m - A = E_g - \Phi_B^p, \tag{2}$$

The injection barriers for the case with interfacial dipole (Fig. 5d and Fig. 6b) are given by Equations 3 and 4, where we consider the case of depositing organic layer on metal (note that the sign of Δ is negative in Fig. 5d and 6b). We see that the injection barrier is modified from the simple expectation of Equations 1 and 2 by Δ. This modification is critically important for applications using carrier injection, such as EL devices[42,43] and spectral sensitization in photography.[35]

$$\Phi_B^p = I - \Phi_m - \Delta, \tag{3}$$

$$\Phi_B^n = \Phi_m - A + \Delta = E_g - \Phi_B^p, \tag{4}$$

When we define slope parameter S as shown in Equation 5, it is unity when the Schottky–Mott rule holds. It is also unity for the case with interfacial dipole layer, when Δ is independent of the metal. On the other hand, if Δ depends on Φ_m, S may deviate from unity. The deviation from unity has often been observed for inorganic semiconductors,[5] and is ascribed to the presence of interface state due to various intrinsic and extrinsic origins.[33,41,44] The values of S range from small (ca. 0.1) for covalent semiconductors like Ge and Si, to nearly 1 for ionic compound semiconductors.[5] Thus the plot of Φ_B^n (or Φ_B^p) vs. Φ_m is useful for examining whether something special occurs at the interface or not.

$$S = d\Phi_B^n / d\Phi_m = -d\Phi_B^p / d\Phi_m, \tag{5}$$

2.4. Practical Factors Affecting the Interfacial Electronic Structure

Before closing the discussion of the conceptual aspects, we call attention to at least two practically important factors in examining the actual interfaces including organics: 1) the possible chemical reaction and diffusion at the interface, and 2) the atmosphere under which the experiments are carried out.

The devices using organic materials are mostly formed by depositing thin layers using techniques such as vacuum deposition and spin-coating. When the metal is deposited on an organic layer by evaporation, the high reactivity of the vaporized hot metal atom often leads to a chemical reaction at the interface.[9,45] Also it is known that metal atoms may diffuse into the organic layer.[46–48] In such cases, the interface cannot be regarded as a simple contact between the metal and the organic layer. Instead, it should be considered as a third layer resulting from reaction and/or diffusion. This is

  0935-9648/99/0806-0611 $ 17.50+.50/0

important since the metal-on-organic system is used in the actual devices, e.g., at the last stage of fabrication of EL devices.[1,2]

In contrast, the situation is usually milder in the case of vacuum deposition of an organic layer on metal substrate, and the interfaces can be often prepared without much diffusion or chemical reaction. Thus the organic-on-metal systems are usually more suitable for studying the basic physical concepts described above, although care must be taken for the possible reaction,[49–52] which may even lead to a complete break in a molecule as suggested for tris(8-hydroxyquinolino)aluminum (Alq_3) on Ca.[51]

Also we note that the atmosphere of the sample fabrication and characterization also affects the observed interfacial electronic structure. When the system is exposed to air or placed in low vacuum, the metal surface is usually oxidized, and adsorption or absorption of molecules like oxygen and water may occur for both the metal and the organic material. In the case of wet film preparation, such as spin-coating, solvents may also remain in the organic film. The actual devices are usually fabricated under such conditions, and significant effects of atmosphere on various electric properties are known.[22,53,54] Further, reactions including these species can also occur.[9,51,55–59] Usually such situations are more severe for polymers than for molecular systems. Together with the possibility of forming special form of charge carriers, such as solitons, polarons, and bipolarons,[60] these factors make the fundamental studies of polymer interfaces rather complex.

On the other hand, basic studies of the organic/metal interface can be more precisely carried out under UHV with in situ sample preparation. This can be performed for molecular material, which can be vacuum-deposited. The situation is more difficult for polymers, but oligomers can be used for such purposes.[9,16,40,57] In the comparison of these results with other experiments, care should be taken to match experimental conditions, and should take into account the possible effects of different atmospheres.

3. Energy Level Alignment at the Interfaces Including Organic Layers

In this section, we survey the present status of understanding about the energy level alignment and electronic structures of the interfaces including organic layers. The subject of band bending will be also briefly discussed.

There are several macroscopic methods, based on electrical measurements, to study the interfacial energy level alignment, such as a) *I–V* characteristics, b) *C–V* characteristics, and c) internal photoemission, which have been developed in studies of inorganic semiconductors.[5,33] Each of these techniques, however, is susceptible to experimental difficulties, and it is wise to compare the results of at least of two of these techniques.[33] Egusa and collaborators developed the displacement current method for examining the injection character and also roughly estimating the barrier height, but its application has so far been limited.[61,62]

In such a situation, a more direct microscopic method is desired, and PEYS has recently been used by many workers.[63] In this technique, the total number of photoelectrons per photon (photoemission yield) is measured as a function of the photon energy.[11,15] Measurements of the metal and the organic layer give the work function of the metal Φ_m and the ionization threshold energy (I) of the organic layer. The hole injection barrier Φ_B^p is estimated as $I - \Phi_m$ (Eq. 1), assuming a common VL as shown in Figure 5c. As mentioned in the preceding section, however, the assumption of a common VL is not generally valid, with possible formation of dipole layer at the interface.

UPS is a powerful technique for studying the electronic structure of material. It has been extensively applied to the studies of various solids and interfaces.[64–66] It is capable of examining the full details of complex interfacial electronic structure, including the possible shift of the VL at the interface. Thus it has been extensively used for studying the interfacial electronic structures of inorganic semiconductors and metals.[33,44]

UPS has also been applied to the studies of the electronic structures of various molecular and polymeric organic materials,[9,15,16,59,66] including the compilation of ionization energies of 120 molecular compounds[15] and about 100 polymers.[16] On the other hand, serious and precise studies of the electronic structure and energy level alignment of organic interfaces, taking account of possible VL shift, have begun just recently.[35,67,68] They are largely stimulated by the rapid development of organic EL devices.[1,2] Thus it is natural that compounds used for EL devices have been mainly examined, but studies of fundamental materials are also important for a deep insight into the mechanisms of energy alignment.

In the following, we focus our attention mainly on the results from molecular systems by UPS. UPS gives the most direct picture about the alignment of the electronic structure between two layers right at the interface. This is described in Section 3.1, and relevant results by other techniques are briefly mentioned in Section 3.2. Also we refer the readers to the literature[9,57] for examples about the current understanding of the interfacial phenomenon and electronic structures of polymers, which are fairly complex due to the factors discussed in Section 2.4.

In Figure 7, we list the structures of the compounds discussed below, on the scale of ionization threshold energy I.[69] For the full names of compounds, see the caption of Figure 7. Since most compounds show optical absorption in the visible region (1.5–3 eV), their HOMO–LUMO gaps are roughly similar. An exception is the long-chain alkane n-$C_{44}H_{90}$, which is a wide-gap insulator. The value of I thus serves as a guide for estimating the electron donating or accepting character of the molecule (Fig. 7). The compounds at the left-hand side are compounds used in EL devices, while those at the right-hand side are other compounds.

  0935-9648/99/0806-0612 $ 17.50+.50/0

ADVANCED MATERIALS

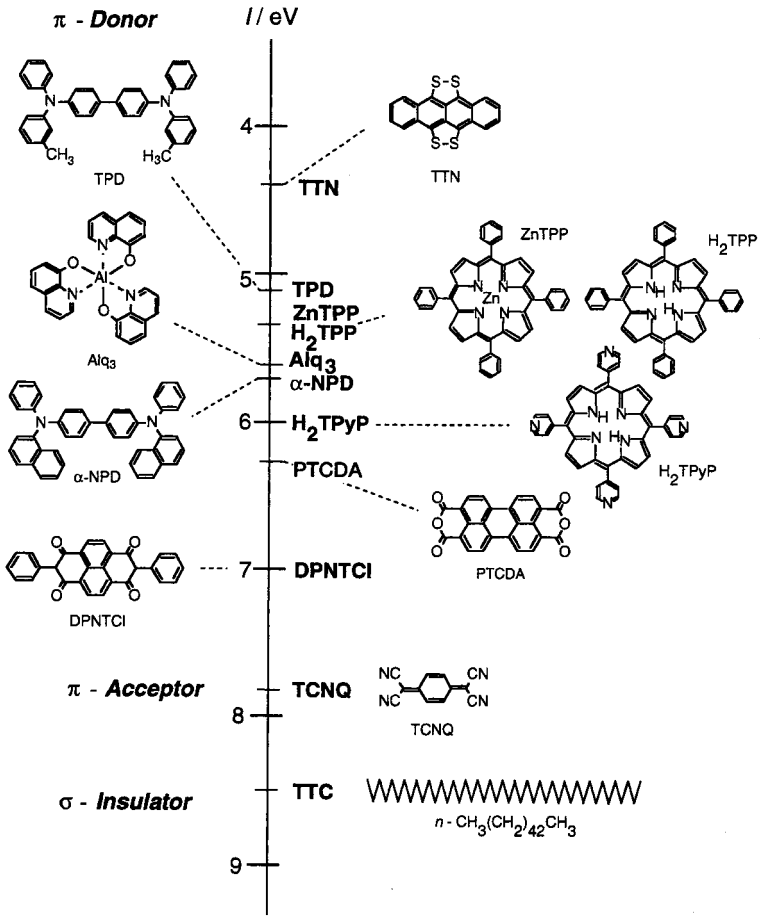

Fig. 7. The structures and ionization threshold energies I (in eV) of organic materials discussed in this paper (modified from previously published work [69], supplemented by the data of PTCDA and α-NPD [39]). The full names of the compounds are: TTN: tetrathianaphthacene, TPD: *N,N′*-diphenyl-*N,N′*-(3-methylphenyl)-1,1′-biphenyl-4,4′diamine, ZnTPP: 5,10,15,20-tetraphenylporphynatozinc(II), H_2TPP: 5,10,15,20-tetraphenylporphyrin, Alq_3: tris(8-hydroxyquinolino)aluminum, α-NPD: *N,N′*-diphenyl-*N,N′*-bis(1-naphthyl)-1,1′-biphenyl-4,4′-diamine, H_2TPyP: 5,10,15,20-tetra(4-pyridyl)porphyrin, PTCDA: perylenetetracarboxylic dianhydride, DP-NTCI: *N,N′*-diphenyl-1,4,5,8-naphthyltetracarboxilicimide, TCNQ: tetracyano-quinodimethane, and TTC: tetratetracontane.

3.1. UPS Studies

3.1.1. Principle of the UPS Study of Interfaces

In UPS, a sample in vacuum is irradiated with high energy monochromatic light, and the energy distribution of emitted electrons (UPS spectrum) is measured. Typical light sources are rare gas discharges and monochromatized synchrotron radiation. The energy analysis is performed with an electrostatic analyzer or a retarding-field analyzer. For other details of the method, see the above-cited references.[64–66] The sample is usually a thin film with tens of nanometers thickness. Thicker samples of nearly insulating organic material may cause charging due to the accumulation of positive charge at the sample surface, which is left by the emission of negatively charged electrons. This factor of charging must be examined for each compound in a trial-and-error manner. Within this limit of thickness, the band bending is generally small, as discussed in Section 2.3.2, and we can assume a flat band in the organic layer as a first-order approximation.

Figure 8 illustrates the principle of UPS and its application to the determination of interfacial electronic state. In Figure 8a, the electronic structure of a metal substrate and the photoemission process are shown. The electrons in the occupied states, with the top at the Fermi level E_F, are excited by the incident light of photon energy $h\nu$, and those with energy above the VL E_{vac}^{m} can escape through the surface. The kinetic energy E_k of photoelectron is given by the Einstein relation

$$E_k = h\nu - E_b \tag{6}$$

where E_b is the binding energy of the electron before excitation relative to the VL. We see that the electron with the maximum kinetic energy E_k^{max}(metal) comes from the excitation from the Fermi level, and the low energy cutoff is defined by the VL E_{vac}^{m}. The work function of the metal Φ_m can be determined from E_k^{max}(metal) by

$$\Phi_m = h\nu - E_k^{max}(\text{metal}) \tag{7}$$

Figure 8b shows the situation when a thin organic layer is deposited on the metal surface. The energy diagram becomes similar to those in Figures 5c and d. Due to the small escape depth (several nanometers) of excited electrons resulting from the scattering in the solid,[64–66] the spectrum becomes dominated by photoelectrons from the organic layer with increasing thickness. Now the electrons with maximum kinetic energy E_k^{max}(org) correspond to the excitation from the HOMO. The energy of the VL may shift from that of the metal substrate, as shown in Figure 5d. This can be observed as the shift Δ of the low energy cutoff of the photoelectron spectra. Thus the origin of the kinetic energy is also changed by this shift of the VL to the VL of the organic layer E_{vac}.

We can derive various physical quantities from these spectra. The ionization threshold energy I of the organic layer is obtained as

$$I = h\nu - E_k^{max}(\text{org}) \tag{8}$$

The energy difference of the fastest electron between the metal and the organic layer gives the energy of the top of the valence state of the organic layer ε_v^F relative to the Fermi level of the metal. This corresponds to the hole injection barrier Φ_B^p, as discussed in Section 2.3.3. In the following, we present the UPS spectra with the energy axis horizontally placed, as shown in Figure 8c. As seen from the correspondence with

  0935-9648/99/0806-0613 $ 17.50+.50/0

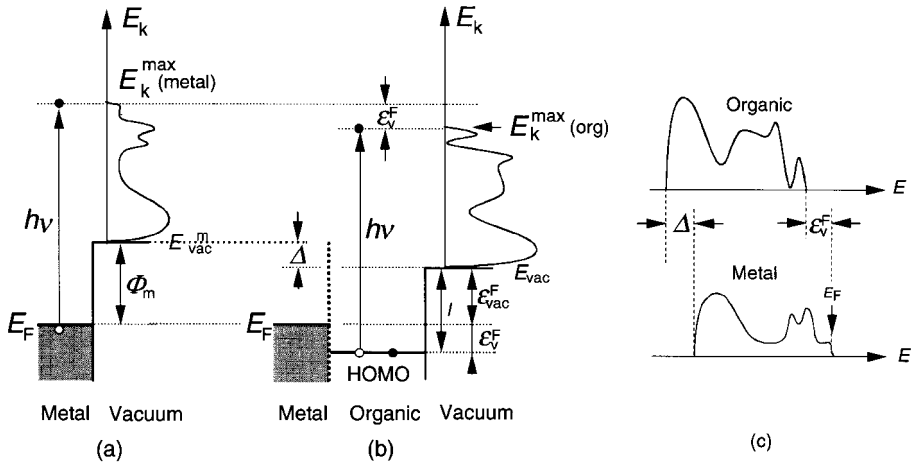

Fig. 8. Principle of the UPS study of an organic/metal interface. a) Photoemission from the metal. b) Photoemission from the organic layer deposited on the metal substrate. c) Presentation of the UPS spectra of metal and organic material with the energy of an emitted electron with an arbitrary origin as the abscissa. $h\nu$: photon energy, E_F: Fermi energy of the metal, Φ_m: work function of the metal, E_{vac}^m: VL of the metal, E_k: kinetic energy of photoelectron, E_k^{max}(metal) maximum kinetic energy of photoelectron from the metal, Δ: VL shift at the interface, HOMO: highest occupied molecular orbital of the organic layer, ε_v^F: energy of the HOMO relative to the Fermi level of the metal, ε_{vac}^F: energy of the VL of the organic layer relative to the Fermi level of the metal, E_{vac}: VL of the organic layer, E_k^{max}(org): maximum kinetic energy of photoelectron form the organic layer.

Figure 8a and Figure 8b, the shift of the right-hand edge gives ε_v^F, while the shift of the left-hand edge gives Δ.

Also the energy of the VL of the organic layer relative to the Fermi level of the metal ε_{vac}^F is obtained as

$$\varepsilon_{vac}^F = I - \varepsilon_v^F. \quad (9)$$

Note that this quantity is not necessarily equal to the work function Φ of the organic layer, since Fermi level alignment is not generally achieved, as discussed in Section 2.3.2.

As can be understood from the description made above, similar studies of organic/organic interface or even multilayer systems can be performed with this technique, although the maximum total thickness is limited by sample charging.

3.1.2. Organic-on-Metal Interfaces

We first examine the results for the interfaces formed by depositing organic material on metals, which are not much troubled by the factor of chemical reaction, as discussed in Section 2.4. Actually, in many cases the UPS spectra show only rigid shifts on the energy scale with a constant value of I, suggesting the absence of strong chemical interaction.[67] Thus we can concentrate on the energy level alignment right at the interface and the interfacial dipole layer formation. Most of this work has been carried out on molecular systems, which can be evaporated, but polymer-related work using an oligomer was also reported.[40] This type of work, including the examination of both the valence band offset ε_v^F and VL shift Δ has been carried out for various combinations of organics and metals.[38–40,42,43,48,51,52,67–88] In most of these reports, the metal substrates were prepared by vacuum deposition under UHV conditions.

As an example, in Figure 9 we show the change of the UPS spectra of clean Au by depositing increasing amounts of *N*,*N*′-diphenyl-*N*,*N*′-(3-methylphenyl)-1,1′-biphenyl-4,4′diamine (TPD), which is a typical material as the HTL in EL devices.[75,78] The light source is a HeI discharge of $h\nu = 21.2$ eV. TPD is a good electron donor (see Fig. 7) with a small ionization threshold energy (5.1 eV),[69] which is desirable for effective hole injection. The right-hand cutoff of clean Au shows the Fermi edge, and the left-hand cutoff corresponds to the VL. By depositing TPD, the emission from Au substrate becomes suppressed, and the spectrum is changed to that of TPD. The right-hand cutoff now corresponds to the HOMO of TPD, and the shift from the Fermi edge of Au gives the relative position of the HOMO from the Fermi level of Au (ε_v^F, see Fig. 8c). The shift of the left-hand cutoff to the left corresponds to the lowering of the VL by the deposition of TPD.

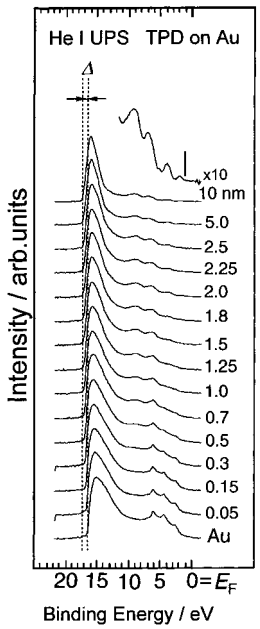

Fig. 9. UPS spectra of TPD incrementally deposited on Au substrate as a function of film thickness [78,81]. The shift of the left-hand cutoff corresponds to the VL shift Δ in Figure 8.

In Figure 10a, we plot the dependence of ε_v^F and ε_{vac}^F on the average film thickness monitored by a quartz oscillator. Initial deposition of TPD induced an abrupt decrease in ε_{vac}^F in the thickness range up to ca. 0.5 nm. The VL is slightly shifted downwards by the further deposition up to about

  0935-9648/99/0806-0614 $ 17.50+.50/0

2 nm thickness, and then becomes almost constant. This shift of the VL by about Δ = –0.5 eV clearly demonstrates the invalidity of the assumption of a common VL and the formation of an interfacial dipole layer, which indicates that we should use Figure 5d rather than 5c. The HOMO energy relative to the Fermi level $\varepsilon_v^F = \Phi_B^p$ also shows film thickness dependence. The HOMO moves downward to about 1.5 nm thickness, and the slope becomes smaller. The ionization threshold energy I corresponds to the sum of ε_v^F and ε_{vac}^F, which is roughly constant, but slightly increases with the thickness. Taking account of the small probing depth of electrons, a possible mechanism of this increase in I is the change in polarization energy (see Sec. 2.1) by an increasing distance from the highly polarizable metal. The barrier height for hole injection Φ_B^p can be estimated to be 0.8 eV by the value of ε_v^F at around monolayer thickness.

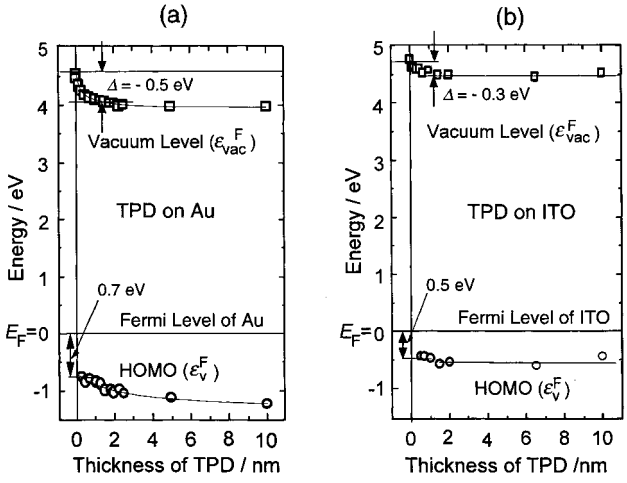

Fig. 10. The thickness dependence of the values of ε_{vac}^F and ε_v^F of TPD film on a) Au and b) ITO substrates [78,81].

A similar shift in the VL was observed when TPD was deposited on indium tin oxide (ITO), which is a typical transparent electrode.[76,78,81] The work function of ITO depends on the cleaning method,[89–93] and needs UV ozone or oxygen plasma treatments for obtaining a work function as large as 4.8 eV, which is advantageous for hole injection.[89–91,93] The deposition of TPD on UV–ozone treated ITO gives the results shown in Figure 10b. The VL is again shifted downwards (about –0.3 eV), with a hole injection barrier of ca. 0.5 eV.

The downward VL shift in these cases makes the hole injection barrier larger than those expected from the simple case without shift shown in Figure 5c. As an extreme case, tetrathianaphthacene (TTN) has smaller ionization threshold energy of 4.3 eV[78,81,94] than the work function of Au (4.7–5.0 eV), and simple considerations predict charge transfer without barrier from TTN to Au. However, the observed large shift in the VL shown in Figure 11 suggests that the HOMO is still lower than the Fermi level of Au, although the precise determination of the location of the HOMO was hindered by the overlap of the strong emission from Au.[78,81] The shift of Δ = ca. –0.5 eV may contain the dipole formed by the electron transfer from TTN, which will lead to the positive charging of the TTN layer and the resultant lowering of its energy levels.

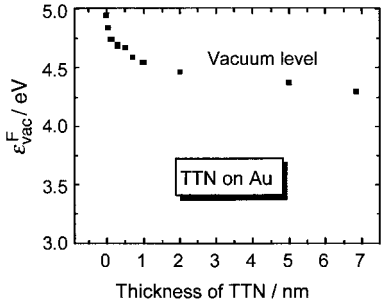

Fig. 11. The thickness dependence of the value of ε_{vac}^F of TTN film on Au substrate [78,81].

The materials for ETL in EL devices generally have electron-accepting properties with large electron affinity (and ionization energy) for effective electron injection. Figure 12a shows the energy diagram of the interface formed by depositing Alq_3 on Al.[70–72,74,78]. Again a large downward shift (Δ = ca. –1.0 eV) is observed. This demonstrates that the interfacial dipole layer can significantly affect the injection efficiency. In Figure 12b the energy diagram without interfacial dipole layer is shown.[78] The injection gap Φ_B^n of more than 1 eV in Figure 12b between E_F and the LUMO is clearly reduced in the case of Figure 12a, although the LUMO energy of Alq_3 cannot be precisely determined from only the optical bandgap of 2.9 eV.

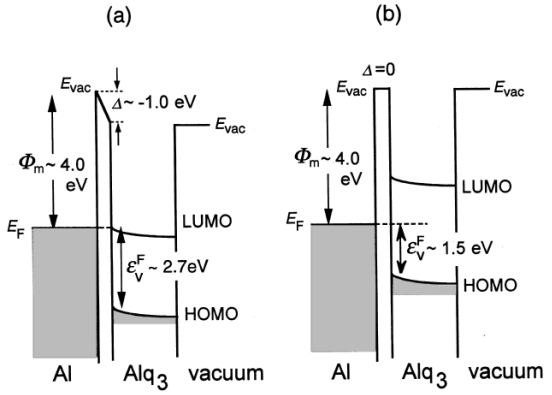

Fig. 12. The interfacial energy diagrams of Alq_3/Al interface obtained from a) UPS and b) the traditional way of estimation [70,78].

The system of Alq_3 on Au was studied by three groups,[39,70,84] and comparison of the results gives an idea of the consistency among different groups (Fig. 13), with another study by scanning tunneling microscopy (STM)-related technique[95,96] to be discussed in Section 3.2.1. The results about ε_v^F (= Φ_B^p) are in reasonable agreement with values of 2.1 eV,[70] 1.75 eV,[84] and 1.8 eV (a few monolayers), and 1.9–2.1 eV (10 nm).[39] The VL lowering also shows reasonable agreement of ca. –1 eV,[70] –1.15 eV,[84] 1.05 eV (a

  0935-9648/99/0806-0615 $ 17.50+.50/0

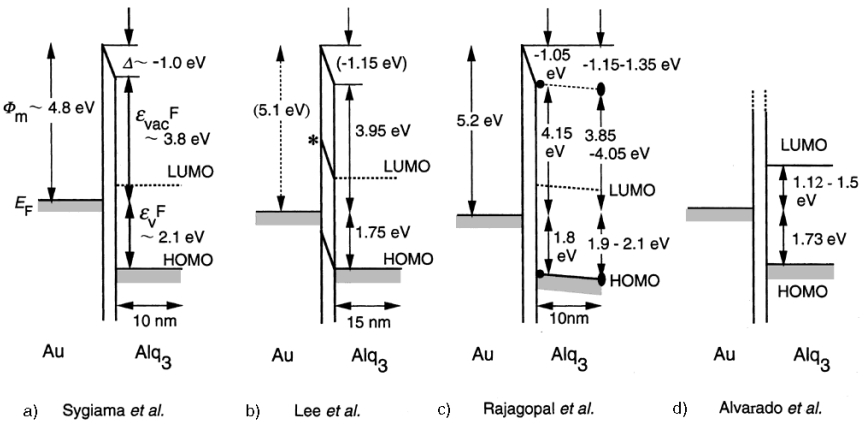

Fig. 13. Comparison of the UPS results for Alq_3 deposited on Au surface. The results from STM measurements are also shown: a) for a molecular layer up to 10 nm [70], b) for a film of 15 nm thick [84], and c) for a film of about monolayer and 10 nm thickness [39]. The results of STM measurements described in Section 3.2.1 are also shown (d) [95,96]. Although the level with * in (b) was used for the estimation of the electron injection barrier [84], it is probably better to use the LUMO energy for this estimation.

few monolayers), and 1.15–1.35 eV (10 nm),[39] although the second value was not directly measured but estimated using the literature value of $\Phi_m = 5.1$ eV.

The deposition of another ETL material *N*,*N*′-diphenyl-1,4,5,8-naphthyltetracarboxilicimide (DP-NTCI) on Au and Al[73,78] shows the change in the sign of the VL shift from negative (–0.7 eV) for Au to positive (+0.4 eV) for Al. This strongly indicates the contribution from the electron transfer to DP-NTCI from Al, which has a smaller work function than Au. This case also shows that we should be careful in using a combination of strong electron acceptor with low work function metal for lowering the barrier height of electron injection. The estimated barrier height is even larger for that of DP-NTCI/Au due to this electron transfer. Similar upward shift of the VL indicative of charge transfer was also found in the case of the stronger acceptor, tetracyanoquinodimethane (TCNQ) on Al and even on Au.[78,81]

The deposition of an insulator with a large bandgap is interesting for examining whether the VL shift can occur without charge transfer or strong chemical interaction. The deposition of a long-chain alkane tetratetracontane (TTC) *n*-$C_{44}H_{90}$ offers such a chance. The results for small alkane molecules indicate that in the first alkane layer is physisorbed without strong chemical interaction.[97] TTC has a large ionization energy of 8.5 eV[98,99] and a small (even negative) electron affinity of –0.5 eV.[100] These values give a large bandgap of 9 eV. The studies of TTC on metals revealed that the shift still exists at the deposition on Au (–0.7 eV), Ag (–0.5 eV), and Pb (–0.3 eV).[77,78] Thus mechanisms other than charge transfer or chemisorption must be operative, as will be discussed in Section 3.1.4.

3.1.3. Organic-on-Organic Interfaces

In multilayer EL devices, organic/organic interface is also important, as in the case of typical layer sequence of Al/Alq_3/TPD/ITO.[1] The deposition of Alq_3 on TPD (which is on ITO) showed little shift of the VL.[78,81] The reversed order of deposition, i.e., TPD on Alq3, was examined by Schlaf et al.[87] in detail by the combination of UPS and XPS, leading also to a small value of $\Delta = -0.05$ eV. On the other hand, the combination of strong donor (TTN) and strong acceptor (TCNQ) gave a VL shift of 0.2–0.3 eV, with the direction corresponding to the dipole polarity of $TTN^{+\delta}TCNQ^{-\delta}$, for both sequences of deposition (TTN on TCNQ and TCNQ on TTN).[78,81] This polarity is in accordance with that expected from the electron-donating and accepting character of these materials. This suggests that electron-transfer can contribute to the dipole layer formation.

Combining the results mentioned above, the whole energy diagram of the device Al/Alq_3/TPD/ITO can be estimated as shown in Figure 14.[76,78,81] We note there is some ambiguity about the interfacial diagram for Al/Alq_3 interface, since it is not estimated by examining the interface formed by depositing Al on Alq_3, but by depositing Alq_3 on Al.

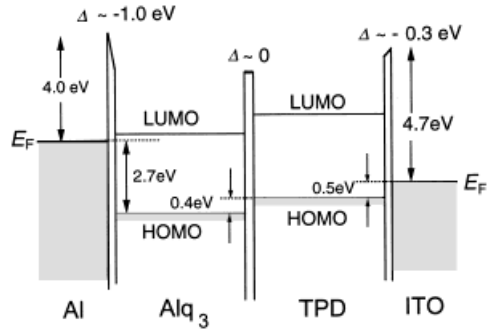

Fig. 14. Energy diagrams of the model interfaces for the Al/Alq_3/TPD/ITO device obtained by UPS [78,81]. Since the behavior of the band bending at the interfaces is unknown, a flat band condition is assumed.

Other combinations of organic/organic interfaces were examined for several systems. Sato and Yoshikawa found a very small Δ (not explicitly given) for chloroaluminum phthalocyanine/*N*,*N*′-dimethylperylene-3,4,9,10-bis(dicarboxylimide).[101] The group of Kahn examined 1) CBP/Alq_3 and CuPC/NPD interfaces (where CuPC = Cu phthalocyanine, CBP = 4,4′-*N*,*N*′-decarbazolylbiphenyl, and (α-NPD) = *N*,*N*′-diphenyl-*N*,*N*′-bis(l-naphthyl)-1,1′-biphenyl-4,4′-diamine),[102] and 2) the combinations among Alq_3, perylene-tetracarboxylic dianhydride (PTCDA), and *N*,*N*′-diphenyl-*N*,*N*′-bis(l-naphthyl)-1,1′-biphenyl-4,4′-diamine (α-NPD).[39,83] The former combinations gave negligible Δ, as expected from the similar donor natures of the materials used. Among the latter combinations, on the other hand, the absolute value of Δ was largest for PTCDA/Alq_3 (0.5 eV with PTCDA negative), while the combination of α-NPD/

  0935-9648/99/0806-0616 $ 17.50+.50/0

PTCDA, which is expected to show a large value according to the donor-acceptor nature, showed only negligible (< 0.1 eV) value. The system of α-NPD/Alq_3 showed deposition-sequence dependence, with the larger value being 0.25 eV for α-NPD deposition. Thus there might be more to the simple picture of charge transfer than meets the eye.

In summary, the presently available data have shown that in most cases the neglect of Δ does not lead to such large errors as in the case of organic/metal interfaces, although in some cases they do exist and further studies are necessary for the accumulation of data in other systems.

3.1.4. Trends in the VL Shift and the Origin of Dipole Layers

After looking at various evidence for the VL Δ at the organic/metal and organic/organic interfaces, we will discuss the trends found in these results, and also discuss the origin of the dipole layer, which is responsible for the shift of the VL.

Ishii and coworkers studied the dependence of Δ on Φ_m for various organic/metal combinations.[38,67,78] The organics include the compounds mentioned above and three porphyrins in Figure 7.[38,67] The results are shown in Figure 15,[78] and two trends are immediately clear: 1) the sign of Δ is mostly negative, corresponding to the lowering of the VL by depositing organic layer on metals; and 2) the shift is mostly a monotonic function of Φ_m, except for the cases where Δ is almost independent of Φ_m.

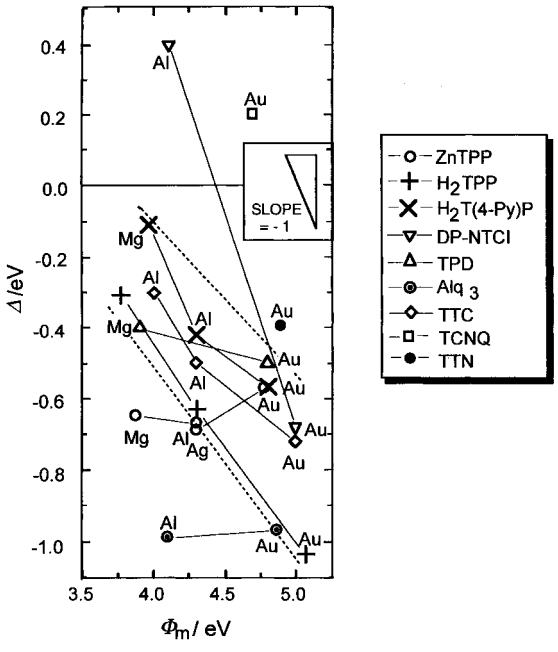

Fig. 15. Plots of the observed VL shift Δ against the work function of the metal Φ_m [78]. The symbols for the organic materials are shown in the right panel. For the structures and the full names of the compounds, see Figure 7 and its caption.

The former corresponds to the positive charging of the vacuum side, since an electron with negative charge feels more comfortable at the positively charged side. The exceptions for this polarity are the combinations of TCNQ/Au, TCNQ/Al, and DP-NTCI/Al, where electron transfer to the acceptor molecule seems to occur, as described in Section 3.1.2. This trend indicates that the traditional method assuming VL alignment (Fig. 5c) tends to underestimate (or overestimate) the hole (electron) injection barrier height. The exceptional case of Δ independent of Φ_m in 2) includes the cases of 5,10,15,20-tetraphenylporphynatozinc(II) (ZnTPP) and Alq_3. Recently Hill et al. also reported similar examination of the Φ_m dependence of Δ for PTCDA, Alq_3, NPD, and CBP.[85] The two trends mentioned above are also seen in their results, although the absolute values are slightly different for the same combinations with those in Figure 15.

On analyzing these results, we should mention four factors depicted in Figure 16a–d even for simple nonpolar molecules mentioned above. The first is the electron transfer between the metal and the organic layer (see Sec. 3.1.2), with the positive and negative charges separated across the interface. This is expected for the combinations of (strong acceptor)—(low work function metal) (Fig. 16a1) and (strong donor)—(high work function metal) (Fig. 16a2). Examples are TCNQ/Au, Al,[78,81] DP-NTCI/Al,[73,78] and PTCDA/Mg, In, Sn[85] for Figure 16a1 and possibly TTN/Au[77,81] and NPD/Au[85] for Figure 16a2. This mechanism should be also operative at organic/organic interfaces for the combination of strong donor and acceptor as described above in Section 3.1.3 for TTN/TCNQ[78] and PTCDA/Alq_3.[39] Another plausible example, although it may be slightly outside of organic materials, is C_{60}. Ohno et al.[103] reported an almost constant value of ε_v^F for various metals, and ascribed this to the charge transfer from the metal into LUMO through weak mixing of the metal wavefunction and the LUMO wavefunction, even claiming that this leads to Fermi level alignment.

There seems to be a trend in the literature to explain VL shifts in terms of such electron transfer between the metal and the molecule. However, VL shifts were observed even for TTCs with a wide HOMO–LUMO gap, where electron transfer is not probable, as described above.[77] This indicates that a dipole layer must be formed.

As the second factor, which may explain such cases, we can mention the image effect or the modification of the surface dipole at metal surface. The results of another good insulator Xe on metals also show VL lowering,[104] and it is ascribed to the polarization of the electron cloud attracted by the image charge formed in the metal.[105] This results in the deficiency of electrons at the vacuum side, leading to a lowering of the VL, as shown in Figure 16b.

There is an alternative explanation about the case of Xe adsorption that the change of the work function is not due to the image effect, but due to the rearrangement of the electron cloud at the metal surface.[106] The tailing part of the electronic cloud into vacuum (Fig. 4b) is pushed back by repulsion with the electron cloud in the adsorbate (Fig. 16c),

  0935-9648/99/0806-0617 $ 17.50+.50/0

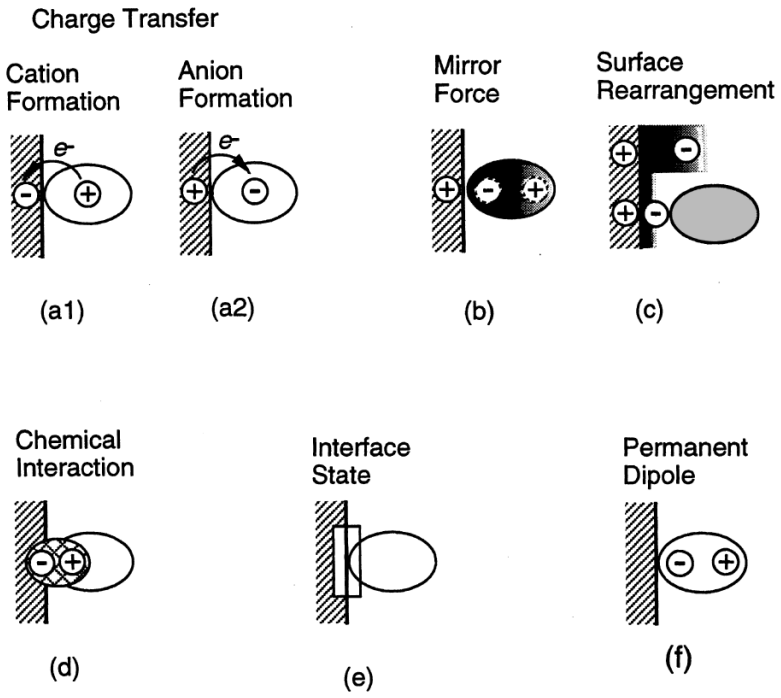

Fig. 16. Possible factors forming and affecting the interfacial dipole layer. a1) and a2): Charge transfer across the interface, b) Concentration of electrons in the adsorbate leading to positive charging of the vacuum side, c) Rearrangement of electron cloud at the metal surface, with the reduction of tailing into vacuum, d) Strong chemical interaction between the surface and the adsorbate leading to the rearrangement of the electronic cloud and also the molecular and surface geometries (both directions of dipoles possible), e) Existence of interface state serving as a buffer of charge carriers, and f) Orientation of polar molecules or functional groups.

resulting in an effectively positive charging of the vacuum side by adsorption compared with the bare surface. This mechanism also leads to the lowering of the VL.

These two mechanisms may also apply to the TTC/metal systems. It should be also applicable to other organic/metal cases, and explains the general trend of VL lowering. When the charge-transfer mechanism shown in Figure 16a1 operates, this will work in a concerted manner with these mechanisms, leading to a downward shift. Charge-transfer interaction in the direction in Figure 16a2 is opposite to that in Figures 16b and c, and an upward shift of the VL is expected only for strong acceptors such as TCNQ, PTCDA, and DP-NTCI.

The third factor is other types of chemical interaction than charge transfer between the organic and metal layers, as depicted in Figure 16d. Various interactions lead to the rearrangement of the chemical bonds, or to the formation of new bonds. Such chemical interaction is well-known for small molecules like CO and benzene on clean metal surfaces.[107] The insensitivity of Δ on Φ_m for Alq_3 in Figure 15 may be due to such interactions as mentioned above. Similar trends for ZnTPP may be also due to such interaction, although the observed UPS spectra do not show the change in the spectral shape. In the case of such chemical interaction, the direction of the dipole depends on the case. Thus the polarity in Figure 16d should not be taken seriously.

The fourth factor is the possible existence of interfacial state. The slope of the Φ_m dependence in Figure 15 corresponds to the slope parameter S for Φ_B^p in Equation 5. The deviation of S from unity corresponds to the variation of Δ with Φ_m, and suggests that there is some mechanism at the interface that works as a buffer at the charge exchange between the metal and the organic layer.[33,41,44] The smaller the value of S, the larger the trend of interface alignment between the Fermi levels of the metal and the organic layer within the interfacial layer. Such interface state is well-known in inorganic semiconductors, and ascribed to various intrinsic and extrinsic origins such as the metal-induced gap states (MIGS) formed by the penetration of metal wavefunctions into semiconductor layer.[33,41,44] Although the origin in the case of organic/metal contact may be much different, there seems to be some analogous mechanism to tune the value of Δ in most of these systems, as depicted schematically in Figure 16e.

Finally we should mention that almost all molecules mentioned above are nonpolar molecules. For polar organic molecules, the orientation of the dipole moment can lead to a large interfacial dipole, as shown in Figure 16f. Possible contribution of this factor was pointed out for merocyanine dye molecules on silver halide surfaces.[35,68] Another example will be discussed in Section 4 in relation to artificial tailoring of Δ.

With these results in mind, we can qualitatively understand the general trend of small values of Δ in organic/organic interfaces described in Section 3.1.3. The mechanisms in Figure 16b–e will be absent in these interfaces, since there are no free electrons causing image charge nor surface dipole due to the large tailing of electron cloud into vacuum as in the case of metal surfaces. Thus we can expect that only the mechanism in Figure 16a will be operative, and the resultant Δ will be small except for the combination of strong electron donor and acceptor pairs such as TCNQ–TTN and PTCDA–Alq_3.

3.1.5. Metal-on-Organic Interfaces

The application of UPS to metal-on-organic systems started from the study of charge-transfer reaction between deposited alkali metals on electron acceptors[108] and the doping of conjugated polymers with alkali metals and other dopants. [109,110] In these cases, the deposited metal atoms often diffuse into the organic layers. By extending such studies, extensive work has been carried out, in particular by Salaneck and coworkers,[9,59] about the systems formed by metal deposition onto conjugated polymers and their

  0935-9648/99/0806-0618 $ 17.50+.50/0

oligomers, which form an important class of materials for EL devices. Complemented by XPS, these studies showed that chemical reaction and metal diffusion can readily occur at many interfaces, as already mentioned in Section 2.4.[9,46–48,55–59,110,111] This is a very important factor at organic interfaces, but makes the analysis of the data rather complex. The detailed characterization of the system was further hindered when the sample is a polymer, which cannot be usually evaporated in situ under UHV.

Partly due to such complex factors, these works did not focus much attention to the energy level alignment right at the interface, even when UPS was employed. Sometimes even a common VL was implicitly assumed. Serious and direct examination of the band offset and VL shift has just started using molecular materials.[48,51,83,84,86,112]

The work of Park et al. about the deposition of Ca on poly(*p*-phenylenevinylene) (PPV) oligomer[112,113] showed a shift in the spectral features to higher binding energy by ca. 0.5 eV and also a change in spectral shape including the appearance of a new feature above the HOMO, which was ascribed to polaron/bipolaron formation. Similar strong metal/organic interaction was observed for the case of Mg on Alq_3,[83,84] which showed a shift in the Alq_3 features to higher binding energy and the appearance of an extra peak above the HOMO of Alq_3 (although Lee et al.[84] did not explicitly mention this peak). The latter may be due to chemical reaction[83] or charge transfer to the LUMO. Such formation of new levels may reduce the hole injection barrier, and are important in the performance of actual devices.[9,82,113,114] Similar change was also found for the Ca/Alq_3 system, but with several stages of chemical interaction.[51] The results of Ag–CBP pair showed no evidence of chemical reaction, as examined by XPS, but both CBP-on-Ag and Ag-on-CBP systems showed downward shifts in the VL.[86] For Mg–CBP[86] and Mg–*p*-sexiphenyl[48] systems, Mg deposited on the organic layers diffuse into the organic layer.

These results for the Mg/Alq_3, Ag/CBP, Mg/CBP, Mg/*p*-sexiphenyl, and Ca/Alq_3 pairs were not symmetric with results for depositing organic materials on a metal, while the results for Au/Alq_3[83] and Au/CBP[86] pairs were symmetric, probably without strong interaction between the two materials. The deposition of Al on *p*-sexiphenyl is reported to be physisorption, with only little VL shift of 0.1 eV,[115] although the metal work function was borrowed from literature.

These results clearly show that metal-on-organic systems are generally much more complex than the organic-on-metal systems, and the results depend on the specific pair. Thus further investigations are necessary for a deeper and more general understanding of these systems.

Finally, we mention that reaction at the deposition of ITO by sputtering on CuPC can be used to obtain a good electron-injecting electrode without using low work function metals.[116] This is somewhat surprising since the system of CuPC/ITO formed by the reversed sequence of deposition is used as a hole-injecting electrode. Parthasarathy et al.[116] suggest that the sputtering should induce many gap states above the Fermi level of ITO, making the electron injection easy.

3.1.6. Effect of Atmosphere

As mentioned in Section 2.4, the electronic properties of organic devices is significantly affected by the atmosphere of preparation and operation.[53,54] Figure 17 shows the results of the examination of the effect of exposure of 10 nm thick ZnTPP film on various metals (Au, Ag, Al, and Mg) to oxygen at 4 torr for 5 min.[38,67] The filled and open circles correspond to the spectra just after in situ vacuum deposition under UHV and those after exposure to O_2 and subsequent re-evacuation to UHV. We see large rigid shifts of the whole spectra, the magnitude and direction of which depend on the metal substrate. This immediately excludes the possibility of O_2 doping of ZnTPP as the major origin of the observed shifts, since the results should not depend on the metal in this case. Rather, these results were ascribed to the oxidation of the metal surface by O_2 molecules arriving at the interface through grain boundaries and other defects. To support this, the directions of the change are consistent with the work function change in the substrate metal materials.[38,67] These results, with shifts of almost 1 eV, clearly demonstrate that the control of atmosphere is crucial for both the fundamental studies of interfaces and the performance of real devices.

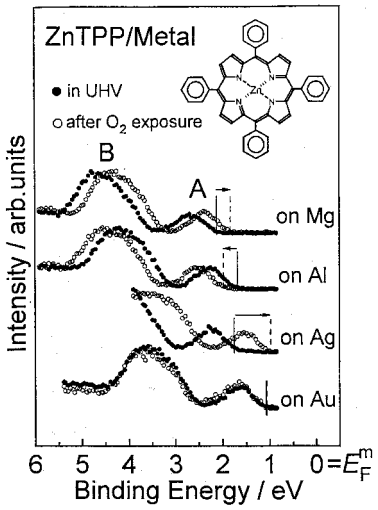

Fig. 17. UPS spectra in the low binding energy region for ZnTPP films evaporated on various metals (Au, Ag, Al, and Mg) in UHV (●) and after exposure to O_2 of 4 torr for 5 min (○) [38,72]. The vertical lines indicate the onsets of peak A.

There is also another report of a rigid shift with a 0.5 eV decrease in ε_v^F at the exposure of *p*-sexiphenyl on stainless steel to O_2 of 330 ML.[117] Supplemented by the 0.3 eV shift of the C1s level by XPS (see Sec. 3.2.1), *p*-type doping of *p*-sexiphenyl was suggested in this case. For more reactive metals, complete oxidation of the metal may occur. The exposure of Ca(30 nm)/PPV oligomer to oxygen (9×10^3 L) was found to remove the metal-induced gap states, and this

  0935-9648/99/0806-0619 $ 17.50+.50/0

was ascribed to the metal oxidation.[118] A similar passivative effect was also found in Ca/Alq_3 system.[51]

3.2. Results by Other Techniques and on Other Organic Systems

Here we discuss results for interfacial electronic structures complementary to those by UPS, particularly with respect to the interfacial energy level alignment.

3.2.1. Other Techniques

There are not much data under UHV by other techniques to be directly compared with the UPS results described above. Still there are some trials as described below.

Using XPS, one can probe the energies of the core levels just as in the case of valence levels in UPS,[64–66] and these energies should reflect the energy level alignment and band bending. Since XPS can be rather easily incorporated with UPS, the combined study of UPS and XPS is a more powerful method than UPS alone. XPS is particularly useful when the organic layer is the substrate, since possible band bending of the organic layer can be probed by virtue of the element-specific nature of the XPS technique. Studies in this direction have been already reported.[57,87,117]

As for STM-related methods, Eisenmenger and collaborators examined the energy level alignment between PTCDA and NTCDA (naphthalenetetracarboxylic dianhydride) on graphite,[119,120] and deduced the band offsets for the HOMO and LUMO. These results, however, are not consistent with those reprted by Kahn and collaborators using UPS and IPES.[20] Recently, Alvarado et al. estimated the barrier height of electron and hole injection from the STM tip into Alq_3 on Au(111) surface by monitoring the tip depth and intensity of injection-induced luminescence as a function of applied voltage at constant-current mode.[95,96] The results are shown in Figure 13d in comparison with the UPS results. The estimated value of 1.12–1.5 eV for the LUMO and 1.73 eV for the HOMO are in reasonable agreement with those by UPS (+ optical bandgap E_g^{opt}). Since the STM results should be mostly free from the excitonic binding energy effect,[22,121] which is involved in the optical bandgap, this apparent agreement may be due to the fortuitous coincidence between the excitonic binding energy C with the sum of the polarization energies (P_+ and P_-) as discussed in Section 2.1.

Also we should mention the estimation of the LUMO energy by IPES.[20,21] In principle it is the most direct method of determining the LUMO energy. Unfortunately, at this stage the resolution is somewhat limited. Also, the direct comparison with the UPS ($+E_g^{opt}$) results is difficult, due to the excitonic effect described above.

The information about unoccupied electronic states can be also obtained from near-edge X-ray absorption fine structure (NEXAFS) spectroscopy,[122] where the excitation of core electrons into various vacant MOs is observed. It has been applied to the study of electronically functional organic materials such as aromatic hydrocarbons,[123,124] fullerenes,[125–127] Alq_3,[128] PPV,[129] and poly(3-methylthiophene).[130] Unfortunately, however, the observed spectrum is usually not a replica of the density of unoccupied states, due to the strong effect of core hole.[122–124,126] Thus it is difficult to use this technique as a direct probe for studying the absolute value of the LUMO energy, and the information is more of qualitative nature such as the detection of charge transfer.[129,130]

There are several examinations of the validity of Schottky–Mott rule for samples under air by electroabsorption and photovoltaic measurements.[131–133] In these measurements, the organic layer is sandwiched between electrodes, and the applied voltage is changed to search for the flat-band condition where either Stark effect on the electronic absorption spectrum[133] or charge separation after photoexcitation (Fig. 1c)[131,132] becomes null. If the Schottky–Mott rule holds, this voltage should be equal to the difference between the work functions of the metal electrodes. The experimental results, obtained under atmospheric conditions, show consistency with this expectation. This means either 1) the charge carriers in the thick organic samples sustain the band bending as shown in Figure 6, or 2) the value of Δ is small or does not depend on the combinations, possibly because of the oxidation of the metal surface.

Internal photoemission was also used for estimating the injection barriers.[133,134] Although there is difficulty as stated in the literature,[33] the results for MEH–PPV (poly[2-methoxy-5-(2′-ethylhexyloxy)-1,4-phenylene vinylene]) under air were reported to be consistent with those of the electroabsorption measurements.[133]

There have been also some studies by Kelvin method for estimating the work function of organic layers.[135–140] Kotani and Akamatu[135,136] carried out pioneering studies of organic solids at the beginning of the 1970s, and the interest in this methods was revived in recent work by Hiramoto et al.[137] An advantage of the Kelvin method is that there is no limitation about film thickness as found in UPS due to sample charging.

Using this method, Pfeiffer et al.[138] reported that the thickness of the diffusion layer (see Fig. 6) for Zn tetraphenylporphyrin is smaller than 50 nm for a film under 5×10^{-5} Pa, while the corresponding value was estimated to be of the order of 100 nm for DTPP00\ (dithioketopyrrolo-{3,4}-pyrrole)[139] and 25 nm for porphyrins[140] in air. Under still higher vacuum, such values may change due to the smaller charge carrier density in the absence of possible dopants such as oxygen, and serious examination of the Fermi level alignment has been required.

An important criterion to examine the Fermi level alignment is that the work function for thick deposited layer on metal does not depend on the metal, since it becomes equal to the work function of the organic layer Φ_{org} (see Fig. 6). Previous studies often claimed the achievement of

  0935-9648/99/0806-0620 $ 17.50+.50/0

ADVANCED MATERIALS

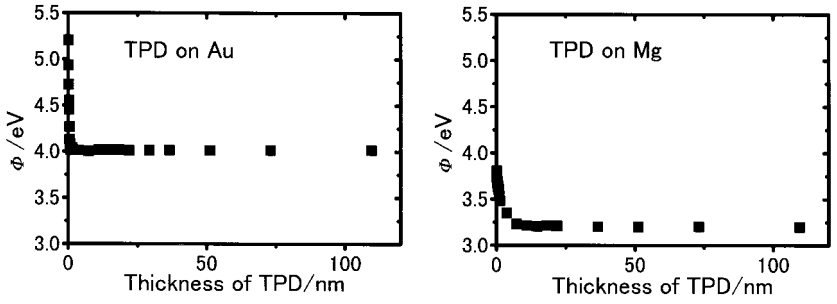

Fig. 18. The energy diagram of a) Alq_3/Al and b) Alq_3/LiF(0.5 nm)/Al interfaces derived from UPS experiments [52].

Fermi level alignment only by observing thickness independence of the energies of the HOMO or VL for a single metal without examining the metal dependence.

In Figure 18 we show our recent examination of the work function in UHV carried out from such a viewpoint.[141] The sample of purified TPD was deposited on freshly evaporated Mg and Au substrates. The reference electrode of the Kelvin probe was always kept in UHV, and its work function Φ_{ref} was calibrated by various metals. As can be seen from Figures 5 and 6, the magnitude of interfacial dipole Δ can be estimated as the change of the work function.

The results of all-UHV measurements for clean substrates in Figure 18 show that most of the work function change is saturated within a rather small average thickness range (<10 nm), and the results agree with those of independent UPS measurements. At further deposition up to 100 nm, the work function shows little variation. Further, the saturated values are definitely different between the cases of Mg substrate (3.22 eV) and Au substrate (4.06 eV).

These results clearly demonstrate the following two important points: 1) the picture of almost flat band in this thickness region described in Section 2.3.2 is valid; and 2) at least for one of these substrates, band bending to achieve Fermi level alignment does not occur.

Thus we can conclude that it is dangerous, at least for well-purified organic materials deposited in UHV, to try to experimentally determine the location of Fermi level at fixed energy, assuming electrical equilibrium with a metal, even for a rather thick organic film.

This kind of measurements can be extended to systems prepared or measured under various atmospheres, combined with other techniques such as electroabsorption or photovoltaic measurements. Such studies will give further insight into the band bending in thick films.

As seen above, all these techniques have advantages complementary to UPS described in Section 3.1, such as the spatial resolution in STM, or the possibility of examining the device under operating conditions in electroabsorption. Further cross examination among various methods with matching of experimental conditions is highly desired.

3.2.2. Other Organic Interfaces

Many UPS studies have been reported about other combinations of organic–metal, organic–semimetal, organic–semiconductor, and organic–ionic solid systems, for example, perylene, PTCDA and thiophene tetramer on Ag(111),[142,143] NTCDA on Ni(111) and O-precovered Ni(111),[144] BTQBT on graphite and MoS_2 (BTQBT: bis(1,2,5-thiadiazolo)-*p*-quinobis(1,3-dithiole)),[145] phthalocyanines on MoS_2, $TaSe_2$, and $MoTe_2$,[146,147] C_{60} on various substrates,[36,148] PTCDA on GaAs(100),[149] titanylphthalocyanine on *n*-TiO_2,[150] and merocyanine dyes on Ag halides.[35] In many of these cases, however, the energy level alignment at the interface was not of primary interest. Even when the alignment was examined, the VL shift was not studied except for in two cases.[35,147] In the first,[35] a detailed study of energy level alignment and the origin of interfacial dipole layer was performed, and the deduced interfacial electronic structure showed excellent correspondence with the sensitizing behaviors of photographic dyes. In the second,[147] a band bending by *n*-type carrier in Cu phthalocyanine was proposed for the interface with $TaSe_2$ based on combined UPS and XPS studies, while little banding by *p*-type carriers was found for the thin interface with $MoTe_2$.

4. Future Prospects and Concluding Remarks

In this article, we have summarized the recent progress in understanding electronic structures at interfaces, including electronically functional large organic molecules and polymers.

These efforts clarified several important factors: 1) the formation of interfacial dipole layer; 2) possible origins of the dipole layer; 3) possible chemical reactions at interface formation; 4) the significant effect of atmosphere on the interfacial electronic structure; and 5) lack of Fermi level alignment at least in some cases. Now we will examine the future directions of the studies of interfaces. There are three major factors.

Firstly, our understanding is not yet sufficient for both interfacial energy level alignment and band bending. Even for energy level alignment, the amount of the experimental data is not yet sufficient for detailed general discussion of the interfacial electronic structures. The results so far obtained have allowed us to see some important empirical trends, but further accumulation of reliable experimental results is necessary for obtaining deeper insight. In this sense, we are now in a comparable stage of research to that in the field of

  0935-9648/99/0806-0621 $ 17.50+.50/0

inorganic semiconductors in the 1940s, when quantitative examinations of the barrier heights were carried out.[5,33,41,44] We have advantages, however, such as knowledge about inorganic systems and well-developed experimental methods.

Furthermore, reliable experimental information about band bending should be carried using a combination of various techniques for a full understanding of the device performance. So far there has been considerable work carried out, in particular by the group of Gao, mainly relying on XPS,[55,56] but parallel studies by UPS and XPS[40,51,147] is highly desirable. Kelvin method, mentioned in Section 3.2.1, will be also useful. For such studies, the control of atmosphere should be extremely important, since the possibility of doping would profoundly affect the observed results. The methods applicable to devices under operation, such as electroabsorption and photovoltaic effect, will be advantageous in clarifying the performance of real devices.

The quality of the experimental data should be also improved. The present situation of the interfacial studies about sample preparation and experimental atmosphere is summarized in Table 1 in comparison with the real device applications and well characterized model systems. The deep understanding of the electronic structure always requires the knowledge of geometrical structures and good characterization of the samples. However, serious studies of the interfacial electronic structures have been largely limited to those formed between deposited polycrystalline metals and amorphous or polycrystalline organic layers. The structure, chemical state, and morphology of these films are in general not well characterized. Also the surface structure and the electronic structure of ITO, which is almost exclusively used as transparent electrode, depends very much on the cleaning method, as described in Section 3.1.2. Undoubtedly one of the most important directions of future research will be a deeper scientific understanding of well-characterized systems. Some trials for the cross characterization of deposited molecular materials by XPS and UPS have already been reported, e.g., for oligomers on Ca[40] and sexiphenyl on metals.[48,115]

A further step towards better characterization will be the use of epitaxially grown organic layer on single crystal surfaces, as shown in Table 1. Since the preparation and characterization of such systems are currently being established,[142–147,149] the combination of electronic probes to these methods should be promising. As an effort in this direction, our recent experiments of epitaxial growth of *n*-$C_{44}H_{90}$ on Cu(100)[78,151] and Au(111)[152] surfaces also showed a VL lowering of –0.33 eV and –0.7 eV for monolayer coverage, respectively.[78] With this kind of information, we can turn to theoreticians for detailed analysis of the observed results, even regarding the interfacial dipole layer.

A second important direction for future studies in relation to the real applications will be the examination of the correspondence between the microscopic observation of interfacial electronic structure and the macroscopic performance, taking special care to match the experimental conditions. One way of matching will be the examination of the electrical and optical measurements under UHV, and the other is the examination of the effect of O_2, H_2O, and other factors in atmospheric conditions, as described in Section 3.1.6.

Finally, the existence of interfacial dipole layer and its effect on energy level alignment suggest the possibility of controlling the energy level alignment with the modification of the interface. An example is the improvement of the performance of EL devices insulating layers at the ETL/cathode interface,[153–155] although the origin is not yet well-clarified. Our recent experiments with Alq_3/LiF/Al system gave the results shown in Figure 19. By inserting a LiF layer, a lowering of the injection barrier by about 0.3 eV was observed,[52] suggesting that a similar lowering in the deposition of Al/LiF/Alq_3 system is a possible origin of enhanced efficiency, although other factors are also proposed.[153] Similar reduction of electron injection barrier was observed by Tokito and collaborators,[88] while Shaheen et al.[156] reported still larger work function lowering of Al by depositing LiF, although they did not examine the deposition of Alq_3 on these modified substrates.

In addition, we found that the deposition of Alq_3 molecules on Al induces an extra occupied state above the HOMO, suggesting a strong chemical interaction between Al and Alq_3.[52] The insertion of LiF eliminated this state.[52] Thus the elimination of strong chemical interaction may be another factor in this case. Huang et al.[157] also suggested such removal of interaction by inserting an insulating layer between Al and Alq_3.

Another good example is the control of interfacial dipole layer by chemical modification of the surface by polar species. This kind of study has been extensively carried out in the field of colloid science,[158] but not much as a tool for improving device performance. A recent report by Campbell et al.[159] demonstrated the control of the work function of Ag by adsorbing polar alkane thiole derivatives with various magnitude and direction of dipole moment to form self-assembled monolayers (SAMs). By using three compounds of various magnitude and direction of dipole moment μ, as shown in Figure 20a–c, they could change the work function by more than 1 eV, with a

Table 1. Comparison of experimental conditions and methods for three typical stages of research on organic/metal interfaces.

		Real application	Current studies		Well-characterized model system
			Molecular	Polymeric	
Organic	method:	evaporated or spin-cast film	evaporated film	spin-coating	evaporated epitaxially grown film
	atmosphere:	low vacuum inert gas under air	UHV	low vacuum inert gas under air	UHV
Metal	method:	evaporated film	evaporated film	evaporated film	atomically clean single crystal
	atmosphere:	low vacuum inert gas under air	UHV	UHV	UHV

0935-9648/99/0806-0622 $ 17.50+.50/0

ADVANCED MATERIALS

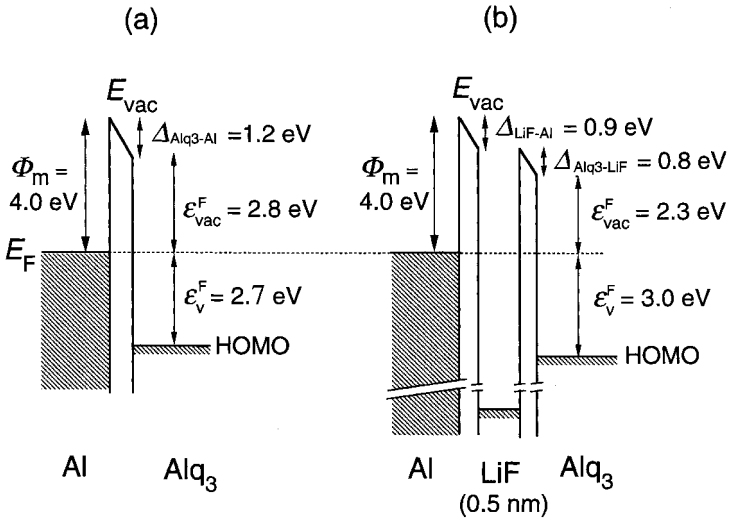

Fig. 19. Change of the work function of metals by the deposition of TPD, measured by the Kelvin method [141]. Metal substrates of Au (a) and Mg (b) were prepared by vacuum deposition in UHV, and TPD was in situ deposited onto it in a stepwise manner. The work function at each step of TPD deposition was carried out in a separated UHV chamber after transfer in UHV, using an electrode with a work function of 4.30 eV calibrated with various metals. The final values are 4.06 eV for Au and 3.22 eV for Mg.

parallel relation with μ, as shown in Figure 20d. They further showed by electroabsorption that the flat-band potential is also modified by almost the same amount.

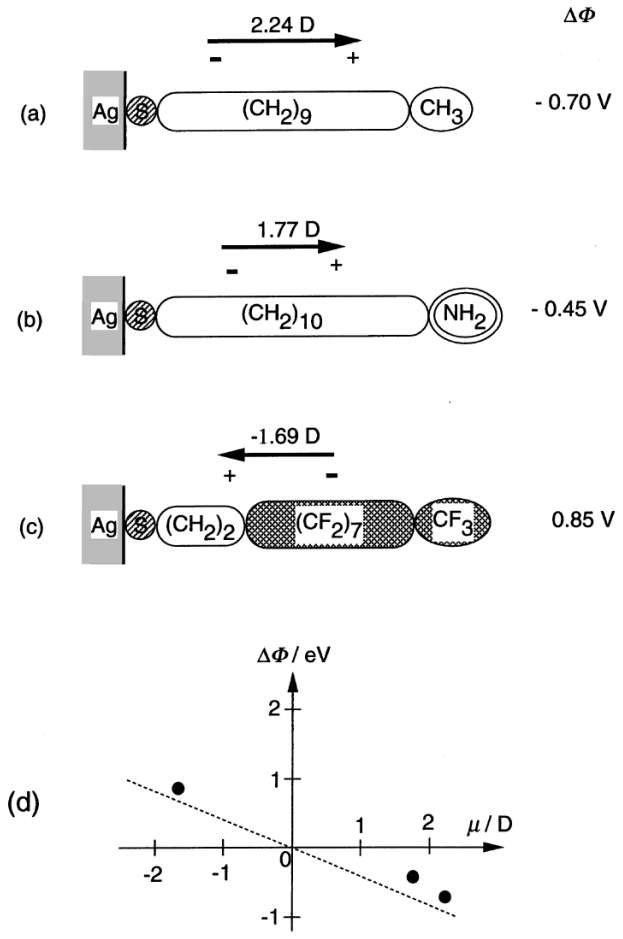

Fig. 20. Surface modification of silver surface by three kinds of self-assembled monolayers with various magnitude and directions of dipoles [159]. a)–c) Structures of the adsorbed monolayer with the dipole moment μ and the shift of the work function of Ag $\Delta\Phi$ by adsorption. d) The correlation between μ and $\Delta\Phi$.

Through these kinds of studies, we will be able to obtain much deeper insight and the way of controlling the electronic structures of organic interfaces to result in better performance of organic electronic devices.

Received: September 21, 1998
Final version: March 15, 1999

Note added in proof: After the completion of the manuscript, the following papers came to our notice, which reflect the vigorous activity in this field. As for the UPS of organic interfaces, many papers were reported for organic/organic,[160] organic/semi-metal,[161] and organic/inorganic-semiconductor[162,163] interfaces, interfaces with LiF layer,[164] and multilayer systems.[165,166] Also the groups of Gao[167] and Salaneck[168] reported new review articles mainly summarizing their work. Band bending was examined in combined UPS and XPS studies,[163] and combined UPS/electrical measurements in UHV were also carried out.[166] Kelvin probe was applied for studying the density of interfacial electronic states at LB film/metals,[169-172] and the built-in potential at polymer/metal interfaces were measured and found to be correlated with metal work function.[173]

[1] C. W. Tang, S. A. VanSlyke, *Appl. Phys. Lett.* **1987**, *51*, 913.
[2] For a review, for example, N. C. Greenham, R. H. Friend, *Semiconductor Device Physics of Conujugated Polymers*, Academic, New York **1995**.
[3] T. Tani, *Photographic Sensitivity*, Oxford University Press, Oxford **1995**.
[4] C. W. Tang, *Appl. Phys. Lett.* **1986**, *48*, 183.
[5] S. M. Sze, *Physics of Semiconductor Devices*, 2nd ed., Wiley, New York **1981**.
[6] I. A. Akimov, V. M. Bentsa, F. I. Vilesov, A. N. Terenin, *Phys. Status Solidi* **1967**, *20*, 771.
[7] Y. Hamada, T. Sano, M. Fujita, T. Fujii, Y. Nishio, K. Shibata, *Jpn. J. Appl. Phys. Pt. 2* **1993**, *32*, L514.
[8] A. Schmidt, M. L. Anderson, N. R. Armstrong, *J. Appl. Phys.* **1995**, *78*, 5619.
[9] W. R. Salaneck, S. Stafström, J. L. Brédas, *Conjugated Polymer Surfaces and Interfaces: Electronic and Chemical Structure of Interfaces for Polymer Light Emitting Devices*, Cambridge University Press, Cambridge **1996**.
[10] K. C. Kao, W. Hwang, *Electrical Transport in Solids*, Pergamon, Oxford **1981**.

  0935-9648/99/0806-0623 $ 17.50+.50/0

[11] F. Gutmann, L. E. Lyons, *Organic Semiconductors*, Wiley, New York **1967**.
[12] C. B. Duke, L. B. Schein, *Phys. Today* **1980**, *33*, 42.
[13] L. E. Lyons, *J. Chem. Soc.* **1957**, 5001.
[14] N. Sato, K. Seki, H. Inokuchi, *J. Chem. Soc. Faraday Trans. 2* **1981**, *77*, 1621.
[15] K. Seki, *Mol. Cryst. Liq. Cryst.* **1989**, *171*, 255.
[16] K. Seki, in *Optical Techniques to Characterize Polymer Systems* (Ed: H. Baessler), Elsevier, Amsterdam **1989**, pp. 115–180.
[17] Riken Keiki Co. Ltd., Azukizawa, Itabashi-ku, Tokyo 174, Japan.
[18] M. L. M. Rocco, K.-H. Frank, P. Yannoulis, E. E. Koch, *J. Chem. Phys.* **1990**, *93*, 6859.
[19] H. M. Meyer III, T. J. Wagener, J. H. Weaver, M. W. Feyereisen, J. Almoloef, *Chem. Phys. Lett.* **1989**, *164*, 527.
[20] C. I. Wu, Y. Hirose, H. Sirringhous, A. Kahn, *Chem. Phys. Lett.* **1997**, *272*, 43.
[21] N. Sato, H. Yoshida, K. Tsutumi, *J. Electron Spectrosc.* **1998**, *88–91*, 65.
[22] J. D. Wright, *Molecular Crystals*, Cambridge University Press, Cambridge **1987**.
[23] L. Apker, E. Taft, J. Dickey, *Phys. Rev.* **1948**, *74*, 1462.
[24] D. P. Woodruff, T. A. Delchar, *Modern Techniques of Surface Science*, Cambridge University Press, Cambridge **1986**.
[25] N. Karl, in *Landolt–Börnstein: Numerical Data and Functional Relation ships in Science and Technology*, Vol. 17i (Eds: O. Madelung, M. Schulz, H. Weiss), Springer, Berlin **1985**, pp. 106–218.
[26] K. Wandelt, in *Thin Metal Films and Gas Chemisorption* (Ed: P. Wissmann), Elsevier, Amsterdam **1987**.
[27] R. A. Strayer, W. Mackie, L. W. Swanson, *Surf. Sci.* **1973**, *34*, 225.
[28] N. Lang, W. Kohn, *Phys. Rev. B* **1970**, *1*, 4555.
[29] N. D. Lang, W. Kohn, *Phys. Rev. B* **1971**, *3*, 1215.
[30] For example, J. C. Slater, N. H. Frank, *Electromagnetism*, McGraw-Hill, New York, **1947**.
[31] J. Hoelzel, F. K. Schulte, H. Wagner, *Solid State Surface Physics*, Springer, Berlin **1979**.
[32] P. Nielsen, *Photogr. Sci. Eng.* **1974**, *18*, 186.
[33] L. J. Brillson, *Surf. Sci. Rep.* **1982**, *2*, 123.
[34] W. Erley, H. Ibach, *Surf. Sci.* **1986**, *178*, 565.
[35] K. Seki, H. Yanagi, Y. Kobayashi, T. Ohta, *Phys. Rev. B* **1994**, *49*, 2760.
[36] G. Gensterblum, K. Hevesi, B.-Y. Han, L.-M. Yu, J.-J. Pireaux, P. A. Thiry, R. Caudano, A.-A. Lucas, D. Bernaerts, S. Amelinckx, G. Van Tendeloo, G. Bendele, T. Buslaps, R. L. Johnson, M. Foss, R. Feidenhansl, G. Le Lay, *Phys. Rev. B* **1994**, *50*, 11 981.
[37] M. Schott, in *Organic Conductors: Fundamentals and Applications* (Ed: P. Farges), Marcel Dekker, New York **1994**, pp. 539–646.
[38] H. Ishii, S. Hasegawa, D. Yoshimura, K. Sugiyama, S. Narioka, M. Sei, Y. Ouchi, K. Seki, Y. Harima, K. Yamashita, *Mol. Cryst. Liq. Cryst.* **1997**, *296*, 427.
[39] A. Rajagopal, C. I. Wu, A. Kahn, *J. Appl. Phys.* **1998**, *83*, 2649.
[40] Y. Park, V. Choong, E. Ettedgui, Y. Gao, B. R. Hsieh, T. Wehrmeister, K. Muellen, *Appl. Phys. Lett.* **1996**, *69*, 1080.
[41] W. Mönch, *Surf. Sci.* **1994**, *299/300*, 928.
[42] K. Sugiyama, D. Yoshimura, E. Ito, T. Miyazaki, Y. Hamatani, I. Kawamoto, Y. Ouchi, K. Seki, *Mol. Cryst. Liq. Cryst.* **1996**, *286*, 239.
[43] H. Ishii, K. Seki, *IEEE Trans. Electron Dev.* **1997**, *44*, 1295.
[44] L. J. Brillson, *Surf. Sci.* **1994**, *299/300*, 909.
[45] N. Uyeda, T. Kobayashi, K. Ishizuka, Y. Fujiyoshi, *Nature* **1980**, *285*, 95.
[46] Y. Hirose, A. Kahn, V. Aristov, P. Soukiassian, *J. Appl. Phys.* **1996**, *68*, 217.
[47] M. J. Tarlov, *Langmuir* **1992**, *8*, 80.
[48] H. Oji, E. Ito, M. Furuta, K. Kajikawa, H. Ishii, Y. Ouchi, K. Seki, *J. Electron Spectrosc.*, in press.
[49] For example, B. G. Frederick, M. R. Ashton, N. V. Richardson, T. S. Jones, *Surf. Sci.* **1993**, *92*, 33.
[50] U. Baston, M. Jung, E. Umbach, *J. Electron Spectrosc.* **1996**, *77*, 75.
[51] V.-E. Choong, M. G. Mason, C. W. Tang, Y. Gao, *Appl. Phys. Lett.* **1998**, *72*, 2689.
[52] D. Yoshimura, E. Ito, H. Ishii, Y. Ouchi, S. Hasegawa, K. Seki, *Synth. Metals*, in press.
[53] Y. Maruyama, H. Inokuchi, *Bull. Chem. Soc. Jpn.* **1966**, *39*, 1418.
[54] M. Martin, J. J. Andre, J. Simon, *J. Appl. Phys.* **1983**, *54*, 2792.
[55] K. Konstadinidis, F. Papadimitrakopoulos, M. Galvin, R. L. Opila, *J. Appl. Phys.* **1995**, *77*, 5642.
[56] K. Xing, M. Fahlman, J. Löglund, D. A. dos Santos, P. V. R. Lazzaroni, J.-L. Brédas, R. W. Gymer, W. R. Salaneck, *Adv. Mater.* **1996**, *8*, 971.
[57] Y. Gao, in *Polymer–Solid Interfaces: from Model to Real Systems* (Eds: J. D. J. J. Pireaux, P. Rudolf), Press Universitaires de Namur, Namur **1998**, p. 365.
[58] V. E. Choong, Y. Park, B. R. Hsieh, Y. Gao, in *Electrical and Optical Polymer Systems: Fundamentals, Methods, and Applications* (Eds: D. L. Wise, G. Wnek, D. J. Trantolo, T. M. Cooper), Marcel Dekker, New York, in press.
[59] M. Löglund, P. Dannetun, W. Salaneck, in *Handbook of Conducting Polymers* (Eds: T. Skotheim, R. L. Elsenbaumer, J. R. Reynolds), Marcel Dekker, New York **1997**, pp. 667–694.
[60] For example, A. J. Heeger, S. Kivelson, J. R. Schrieffer, W.-P. Su, *Rev. Mod. Phys.* **1988**, *60*, 781.
[61] S. Egusa, N. Gemma, A. Miura, K. Mizushima, M. Azuma, *J. Appl. Phys.* **1992**, *71*, 2042.
[62] K. Yamamoto, S. Egusa, M. Sugiuchi, A. Miura, *Solid State Commun.* **1993**, *85*, 5.
[63] For example, T. Sano, Y. Hamada, K. Shibata, *IEEE J. Select. Top. Quant. Electron.* **1998**, *4*, 34.
[64] L. Ley, M. Cardona, *Photoemission in Solids.*, Vol. 1 and 2, Springer, Berlin **1978/1979**.
[65] S. Hüfner, *Photoelectron Spectroscopy*, 2nd ed., Springer, Berlin **1996**.
[66] W. D. Grobman, E. E. Koch, in *Photoemission in Solids*, Vol. 2 (Eds: L. Ley, M. Cardona), Springer, Berlin **1979**, pp. 261–298.
[67] S. Narioka, H. Ishii, D. Yoshimura, M. Sei, Y. Ouchi, K. Seki, S. Hasegawa, T. Miyazaki, Y. Harima, K. Yamashita, *Appl. Phys. Lett.* **1995**, *67*, 1899.
[68] K. Seki, T. Tani, H. Ishii, *Thin Solid Films* **1996**, *273*, 20.
[69] K. Sugiyama, D. Yoshimura, T. Miyamae, T. Miyazaki, H. Ishii, Y. Ouchi, K. Seki, *J. Appl. Phys.* **1998**, *83*, 4928.
[70] K. Sugiyama, D. Yoshimura, E. Ito, T. Miyazaki, Y. Hamatani, I. Kawamoto, Y. Ouchi, K. Seki, *Mol. Cryst. Liq. Cryst.* **1996**, *286*, 239.
[71] K. Sugiyama, D. Yoshimura, E. Ito, T. Miyazaki, Y. Hamatani, I. Kawamoto, H. Ishii, Y. Ouchi, K. Seki, *Synth. Metals* **1997**, *86*, 2425.
[72] H. Ishii, K. Seki, *IEEE Trans. Electron Dev.* **1997**, *44*, 1295.
[73] H. Ishii, K. Sugiyama, K. Seki, *Proc. SPIE Int. Symp. Organic Light-Emitting Materials and Devices*, San Diego **1997**, 228.
[74] K. Seki, E. Ito, H. Ishii, *Synth. Metals* **1997**, *91*, 137.
[75] K. Seki, H. Ishii, *J. Electron Spectrosc.* **1997**, *88–91*, 821.
[76] K. Sugiyama, K. Seki, E. Ito, Y. Ouchi, H. Ishii, *Proc. Materials Research Society on Electrical, Optical, and Magnetic Properties of Organic Solid-State Materials IV*, Vol. 488, Materials Research Society, Boston **1997**, p. 719.
[77] E. Ito, H. Oji, H. Ishii, K. Oichi, Y. Ouchi, K. Seki, *Chem. Phys. Lett.* **1998**, *287*, 137.
[78] H. Ishii, K. Sugiyama, D. Yoshimura, E. Ito, Y. Ouchi, K. Seki, *IEEE J. Sel. Top. Quant. Electron.* **1998**, *4*, 24.
[79] H. Ishii, D. Yoshimura, E. Ito, K. Okudaira, T. Miyamae, S. Hasegawa, N. Ueno, K. Seki, *J. Electron Spectrosc.*, in press.
[80] D. Yoshimura, E. Ito, H. Ishii, Y. Ouchi, S. Hasegawa, K. Seki, *Synth. Metals*, in press.
[81] K. Sugiyama, unpublished results.
[82] A. Rajagopal, A. Kahn, *Adv. Mater.* **1998**, *10*, 140.
[83] A. Rajagopal, A. Kahn, *J. Appl. Phys.* **1998**, *84*, 355.
[84] S. T. Lee, X. Y. Hou, M. G. Mason, C. W. Tang, *Appl. Phys. Lett.* **1998**, *72*, 1593.
[85] I. G. Hill, A. Rajagopal, A. Kahn, Y. Hu, *Appl. Phys. Lett.* **1998**, *73*, 662.
[86] I. G. Hill, A. Rajagopal, A. Kahn, *J. Appl. Phys.* **1998**, *84*, 3236.
[87] R. Schlaf, B. A. Parkinson, P. A. Lee, K. W. Nebesny, N. R. Armstrong, *Appl. Phys. Lett.* **1998**, *73*, 1026.
[88] T. Mori, H. Fujikawa, S. Tokito, Y. Taga, *Appl. Phys. Lett.* **1998**, *73*, 2763.
[89] T. Kugler, A. Johannson, I. Dalsegg, U. Gelius, W. R. Salaneck, *Synth. Met.* **1997**, *91*, 143.
[90] C. C. Wu, C. I. Wu, J. C. Sturm, A. Kahn, *Appl. Phys. Lett.* **1997**, *70*, 1348.
[91] A. Bernsten, Y. Croonen, R. Cuijpers, B. Habets, C. Liedenbaum, H. Schoo, F. J. Visser, J. Vleggaar, P. van de Weijer, *Organic Light-Emitting Materials and Devices, part of SPIE–Int. Soc. Opt. Eng.*, San Diego **1997**.
[92] Y. Park, V. Choong, Y. Gao, B. R. Hsieh, C. W. Tang, *Appl. Phys. Lett.* **1996**, *68*, 2699.
[93] K. Sugiyama, H. Ishii, K. Ouchi, K. Seki, unpublished results.
[94] N. Sato, I. Shirotani, H. Inokuchi, *Chem. Phys.* **1981**, *60*, 327.
[95] S. F. Alvarado, L. Libioulee, P. F. Seidler, *Synth. Met.* **1997**, *91*, 69.
[96] S. F. Alvarado, private communication.
[97] B. A. Sexton, A. E. Hughes, *Surf. Sci.* **1994**, *140*, 227.
[98] M. Fujihira, H. Inokuchi, *Chem. Phys. Lett.* **1972**, *17*, 554.

  0935-9648/99/0806-0624 $ 17.50+.50/0

[99] K. Seki, N. Ueno, unpublished results.
[100] N. Ueno, K. Sugita, K. Seki, H. Inokuchi, *Phys. Rev. B* **1986**, *34*, 6386.
[101] N. Sato, M. Yoshikawa, *J. Electron Spectrosc.* **1996**, *78*, 387.
[102] I. G. Hill, A. Rajagopal, A. Kahn, *J. Appl. Phys.* **1998**, *84*, 5583.
[103] T. R. Ohno, Y. Chen, S. E. Harvey, G. H. Kroll, J. H. Weaver, R. E. Haufler, R. E. Smalley, *Phys. Rev. B* **1991**, *44*, 13 747.
[104] A. Zangwill, *Physics at Surfaces*, Cambridge University Press, Cambridge **1988**.
[105] K. Wandelt, J. E. Hulse, *J. Chem. Phys.* **1984**, *80*, 1340.
[106] W. Widdra, private communication.
[107] H. J. Freund, H. Kuhlenbeck, in *Application of Synchrotorn Radiation* (Ed: W. Eberhardt), Springer, Berlin **1995**, pp. 9–60.
[108] W. D. Grobman, R. A. Pollak, D. E. Eastman, E. T. Maas Jr., B. A. Scott, *Phys. Rev. Lett*. **1974**, *32*, 534.
[109] J. Lee, C. Hanrahan, J. Arias, R. M. Martin, H. Metiu, *Phys. Rev.* **1985**, *B32*, 8216.
[110] P. Dannetum, M. Boman, S. Stafström, W. R. Salaneck, R. Lazzaroni, C. Fredriksson, L. J. Brédas, R. Aamboni, C. Taliani, *J. Chem. Phys.* **1993**, *99*, 664.
[111] Y. Hirose, A. Kahn, V. Aristov, P. Soukiassian, *J. Appl. Phys.* **1996**, *68*, 217.
[112] Y. Park, E. Ettedgui, Y. Gao, B. R. Hsieh, K. Müllen, *Polym. Prepr.* **1995**, *36*, 382.
[113] V. E. Choong, Y. Park, B. R. Hsieh, Y. Gao, *Phys. Rev. B* **1997**, *55*, 15 460.
[114] W. R. Salaneck, J. L. Brédas, *Adv. Mater.* **1996**, *8*, 48.
[115] N. Koch, L. M. Yu, P. V. R. Lazaaroni, R. L. Johnson, G. Leising, J. J. Pireaux, J. L. Bredas, *Adv. Mater.* **1998**, *10*, 1038.
[116] G. Parthasarathy, P. E. Burrows, V. Khalfin, V. G. Kozlov, S. R. Forrest, *Appl. Phys. Lett.* **1998**, *72*, 2138.
[117] N. Koch, L.-M. Yu, J.-L. Guyaux, Y. Morciaux, G. Leising, J.-J. Pireaux, G. Demoustier, in *Proc. Materials Research Society on Electrical, Optical, and Magnetic Properties of Organic Solid-State Materilas IV*, Vol. 488, (Eds: J. R. Reynolds, A. K.-Y. Jen, J. F. Rubner, L. Y. Chiang, L. R. Dalton), Materials Research Society, Boston **1997**, p. 509.
[118] Y. Park, V. E. Choong, B. R. Hsieh, C. W. Tang, Y. Gao, *Phys. Rev. Lett.* **1997**, *78*, 3955.
[119] C. Ludwig, B. Gompf, J. Peterse, R. Strohmaier, W. Eisenmenger, *Z. Phys.* **1994**, *B93*, 365.
[120] P. Strohmaier, C. Ludwig, J. Petersen, B. Gompf, W. Eisenmenger, *Surf. Sci.* **1996**, *351*, 292.
[121] S. F. Alvarado, P. F. Seidler, D. G. Lidzey, D. D. C. Bradley, *Phys. Rev. Lett.* **1998**, *81*, 1082.
[122] J. Stöhr, *NEXAFS Spectroscopy*, Springer, Berlin **1992**.
[123] T. Yokoyama, K. Seki, I. Morisada, K. Edamatsu, T. Ohta, *Phys. Scr.* **1990**, *41*, 189.
[124] H. Oji, R. Mitsumoto, E. Ito, H. Ishii, Y. Ouchi, K. Seki, T. Yokoyama, T. Ohta, N. Kosugi, *J. Chem. Phys.*, in press.
[125] C. T. Chen, L. H. Tjeng, P. Rudolf, G. Meigs, J. E. Rowe, J. Chen, P. P. McCauley Jr., A. B. Smith III, A. R. McGhie, W. J. Romanow, E. W. Plummer, *Nature* **1991**, *352*, 603.
[126] K. Seki, R. Mitsumoto, T. Araki, E. Ito, Y. Ouchi, K. Kikuchi, Y. Achiba, *Synth. Met.* **1994**, *64*, 353.
[127] M. S. Dresselhaus, G. Dresselhaus, P. C. Eklund, *Science of Fullerenes and Carbon Nanotubes*, Academic, San Diego, CA **1996**.
[128] A. Curioni, W. Andreoni, R. Treusch, F. J. Himpsel, E. Haskal, P. Seidler, C. Heske, S. Kakaer, T. van Buuren, L. J. Terminello, *Appl. Phys. Lett.* **1998**, *72*, 1575.
[129] R. Ettedgui, H. Y. Gao, B. R. Hsieh, W. A. Feld, M. W. Ruckman, *Phys. Rev. Lett.* **1996**, *76*, 299.
[130] G. Tourillon, A. Fontaine, Y. Jugnet, T. M. Duc, W. Braun, J. Feldhaus, E. Holub-Krappe, *Phys. Rev. B* **1987**, *36*, 3483.
[131] Y. Harima, H. O. T. Kodaka, Y. Kunugi, K. Yamashita, H. Ishii, K. Seki, *Chem. Phys. Lett.* **1995**, *240*, 345.
[132] Y. Harima, Y. K. H. Okazaki, K. Yamashita, H. Ishii, K. Seki, *Appl. Phys. Lett.* **1996**, *69*, 1059.
[133] I. H. Campbell, T. W. Hagler, D. L. Smith, *Phys. Rev. Lett.* **1996**, *76*, 1900.
[134] G. L. J. A. Rikken, D. Braun, E. G. J. Staring, R. Demandt, *Appl. Phys. Lett.* **1994**, *65*, 219.
[135] M. Kotani, H. Akamatu, *Bull. Chem. Soc. Jpn.* **1970**, *43*, 30.
[136] M. Kotani, H. Akamatu, *Disc. Faraday Soc.* **1971**, *51*, 94.
[137] M. Hiramoto, K. Ihara, M. Yokoyama, *Jpn. J. Appl. Phys.* **1995**, *34*, 3803.
[138] M. Pfeiffer, K. Leo, N. Karl, *J. Appl. Phys.* **1996**, *80*, 6880.
[139] M. Eschle, E. Moons, M. Grätzel, *Opt. Mater.* **1998**, *9*, 138.
[140] E. Moons, A. Goossons, T. Savenije, *J. Phys. Chem.* **1997**, *B101*, 8492.
[141] N. Hayashi, E. Ito, H. Ishii, Y. Ouchi, K. Seki, unpublished results.
[142] M. Jung, U. Baston, G. Schnitzler, M. Kaiser, J. Papst, T. Porwol, H. J. Freund, E. Umbach, *J. Mol. Struct.* **1993**, *293*, 239.
[143] U. Baston, M. Jung, E. Umbach, *J. Electron Spectrosc.* **1996**, *77*, 75.
[144] A. Soukopp, C. Seidel, R. Li, M. Baessler, M. Sokolowski, E. Umbach, *Thin Solid Films* **1996**, *284–285*, 343.
[145] N. Ueno, A. Kitamura, K. K. Okudaira, T. Miyamae, S. Hasegawa, H. Ishii, H. Inokuchi, T. Fujikawa, T. Miyazaki, K. Seki, *J. Chem. Phys.* **1997**, *107*, 2079.
[146] N. Ueno, *J. Electron Spectrosc.* **1996**, *78*, 345.
[147] T. Shimada, K. Hamaguchi, A. Koma, F. S. Ohuchi, *Appl. Phys. Lett.* **1998**, *72*, 1869.
[148] J. H. Weaver, D. M. Poirier, *Solid State Phys.* **1994**, *48*, 1.
[149] Y. Hirose, Q. Chen, E. I. Haskal, S. R. Forrest, A. Kahn, *Appl. Phys. Lett.* **1994**, *64*, 3482.
[150] H. Yanagi, S. Chen, P. A. Lee, K. W. Nebesny, N. R. Armstrong, A. Fujishima, *J. Phys. Chem.* **1996**, *100*, 5447.
[151] D. Yoshimura, H. Ishii, Y. Ouchi, E. Ito, T. Miyamae, S. Hasegawa, N. Ueno, K. Seki, *J. Electron Spectrosc.* **1998**, *88–91*, 875.
[152] H. Ishii, unpublished results.
[153] Y. Kim, H. Park, J. Kim, *Appl. Phys. Lett.* **1996**, *69*, 599.
[154] L. S. Hung, C. W. Tang, M. G. Mason, *Appl. Phys. Lett.* **1997**, *70*, 152.
[155] F. Li, H. Tang, J. Anderegg, J. Shinar, *Appl. Phys. Lett.* **1997**, *70*, 1233.
[156] S. E. Shaheen, G. E. Jabbour, M. M. Morrell, Y. Kawabe, B. Kippelen, N. Peyghambarian, M.-F. Nabor, R. Schlaf, E. A. Mash, N. R. Armstrong, *J. Appl. Phys.* **1998**, *84*, 2324.
[157] M. B. Huang, K. McDonald, J. C. Keay, Y. Q. Wang, S. J. Rosenthal, R. A. Weller, L. C. Feldman, *Appl. Phys. Lett*. **1998**, *73*, 2914.
[158] A. Ulman, *An Introduction to Ultrathin Organic Films: from Langmuir–Blodgett to Self-assembly*, Academic, San Diego, CA **1991**.
[159] I. H. Campbell, T. A. Z. S. Rubin, J. D. Kress, R. L. Martin, D. L. Smith, N. N. Barashkov, J. P. Ferraris, *Phys. Rev. B* **1996**, *54*, R14 321.
[160] R. Schlaf, B. A. Parkinson, P. A. Lee, K. W. Nebesny, N. R. Armstrong, *J. Phys. Chem.* **1999**, *103*, 2984.
[161] R. Schlaf, B. A. Parkinson, P. A. Lee, K. W. Nebesny, N. R. Armstrong, *Surf. Sci. Lett.*, in press.
[162] T. Chasse, C.-I. Wu, I. G. Hill, A. Kahn, *J. Appl. Phys.* **1999**, *85*, 6589.
[163] R. Schlaf, P. G. Schroeder, M. W. Nelson, B. A. Parkinson, P. A. Lee, K. W. Nebesny, N. R. Armstrong, private communication.
[164] R. Schlaf, B. A. Parkinson, K. W. Nebesny, G. Jabbour, B. Kippelen, N. Peyghambarian, N. R. Armstrong, *J. Appl. Phys.* **1998**, *84*, 6729.
[165] S. T. Lee, Y. M. Wang, X. Y. Hou, C. W. Tang, *Appl. Phys. Lett.* **1999**, *74*, 670.
[166] I. G. Hill, A. Kahn, private communication.
[167] Y. Gao, *Acc. Chem. Res.* **1999**, *32*, 247.
[168] T. Kugler, M. Loeglund, W. R. Salaneck, *Acc. Chem. Res.* **1999**, *32*, 225.
[169] E. Itoh, M. Iwamoto, *J. Appl. Phys.* **1997**, *81*, 1790.
[170] E. Itoh, H. Kokubo, M. Iwamoto, M. Burghard, S. Roth, M. Hanack, *Jpn. J. Appl. Phys.* **1998**, *37*, 577.
[171] T. Kubota, S. Kuragasaki, M. Iwamoto, *Jpn. J. Appl. Phys.* **1998**, *37*, Pt. 1, 4428.
[172] E. Itoh, H. Kokubo, S. Shouriki, M. Iwamoto, *J. Appl. Phys.* **1998**, *83*, 372.
[173] C. M. Heller, I. H. Campbell, D. L. Smith, N. N. Barashkhov, J. P. Ferraris, *J. Appl. Phys.* **1997**, *81*, 3227.

  0935-9648/99/0806-0625 $ 17.50+.50/0